



Research Internship (PRE)

Applied Mathematics
2023-2024

Non-selfadjoint periodic Schrödinger operators: numerics and conjectures.

NOT CONFIDENTIAL

Lucie Levadoux, Student at ENSTA Paris

Under the supervision of:
Marco Marletta,
Professor at Cardiff University,
Head of Analysis Group

Academic advisor:
Sonia Fliss,
Professor at ENSTA Paris,
Researcher at POEMS (UMA)

13th May 2024 - 12th August 2024
Cardiff University, School of Mathematics
Abacws, Senghenydd Road, Cathays, Cardiff, CF24 4AG

Acknowledgments

I would like to express my sincere gratitude to Mr. Marletta for proposing this well-suited research topic for my internship and for his encouragement and guidance throughout the three months I stayed in Cardiff. His efforts to organize meetings to monitor my progress, answer my questions, and satisfy my curiosity were greatly appreciated.

I am also deeply grateful to my academic advisor, Sonia Fliss, for her assistance in finding the internship and connecting me with Mr. Marletta to secure a topic that aligned with my expectations.

Finally, I extend my heartfelt thanks to the professors at ENSTA —Anne-Sophie Bonnet-Ben Dhia, Christophe Hazard, and Jean-François Mercier —for the ANA202 Spectral Theory course, which I thoroughly enjoyed and was able to apply during this internship.

Abstract

These notes are dedicated to the study of Schrödinger operators with a periodic complex potential, also known as Hill operators. The purpose is to examine the question of space-filling spectrum for such operators when the potential is complex and the most efficient ways to compute it numerically.

Keywords:
Spectrum, Schrödinger operator, Floquet-Bloch, periodic, non-selfadjoint.

CONTENTS

Contents

Acknowledgements	2
Abstract	3
1 Introduction	5
2 First steps in 1D	5
2.1 Floquet-Bloch transform	6
2.2 How to obtain $\sigma(H_k)$?	6
2.3 First experiments	10
3 First steps in 2D	14
3.1 Floquet-Bloch transform	15
3.2 How to obtain $\sigma(H_{k_1, k_2})$?	15
3.3 First experiments	17
4 Some ideas of improvements	20
4.1 Finding good values of k	20
4.2 Identifying the connected components $\lambda_n(\mathcal{B}_{2D})$	23
A Floquet theory	33
B Hill discriminant	34
C Special Case in 2D: $V(x_1, x_2) = V_1(x_1) + V_2(x_2)$	36
D Kronecker product	38
Bibliography	39

1 Introduction

This report is the synthesis of work carried out as part of the research project that concludes the second year of the ENSTA (Applied Mathematics track) program. Supervised by Professor M. Marletta, head of the Analysis group in the Mathematics Department at Cardiff University, it took place over a period of 13 weeks, from May to August 2024.

The topic proposed to me concerns the study of the spectrum of operators derived from quantum mechanics. More specifically, it involves Schrödinger operators with periodic potentials, which are particularly relevant in solid-state physics for describing the dynamics of electrons in a crystal through the probability wave function. The eigenvalues then correspond to the different energy levels that can exist within the crystal.

The spectrum of these operators is well known in the case of real potentials. In this case, the spectrum coincides with a union of bands on the real axis. The properties of these bands vary significantly depending on the dimensionality of the problem. In the one-dimensional case, these bands become increasingly longer, and the gaps between them decrease rapidly, but the number of gaps remains infinite. In the case of a 2D or 3D lattice, the band structure is more complex. The bands can overlap, and the gaps between them may be reduced or even disappear entirely, leading to a continuous spectrum rather than distinct bands. Conjectured in the 1930s by the physicists A. Sommerfeld and H. Bethe, it is now proved since 2007 that the number of gaps in higher dimensions than one is always finite.

My task was to focus on the non-selfadjoint case, for which there are significantly fewer results available. Developing numerical methods for the rapid calculation of such spectra is important for formulating or disproving new conjectures. In the 1D case, I observed that introducing a complex potential does not make it more difficult to obtain the spectrum, as it still consists of bands (although they are displaced from the real axis) with boundaries that are relatively easy to determine. However, in the 2D case discussed in the second part, introducing a complex potential profoundly changes the nature of the spectrum. It is no longer composed of bands but rather of surfaces, and the contours of these surfaces are very challenging to delineate.

A close examination of Floquet theory reveals that the parameter space (known in physics as the Brillouin zone) is not optimal from a mathematical perspective. Additionally, a naive discretization of this space risks providing an incomplete representation of the spectrum. Consequently, a very fine discretization step is required, which can lead to significant computation times. From a restricted parameter space, I have attempted to implement more effective exploration methods. Furthermore, paying attention to the intrinsic properties of the potential of the studied operator allows for the identification of simpler cases to address.

2 First steps in 1D

We want to compute the spectrum of the Hill operator

$$H = -\frac{d}{dx^2} + V(x)$$

where $V : \mathbb{R} \rightarrow \mathbb{C}$ is a -periodic and bounded.

The domain of our operator H is the Sobolev space $H^2(\mathbb{R})$.

Remark 1

When V is real, it can be shown that H is selfadjoint. (see (1))

2.1 Floquet-Bloch transform

According to the Floquet-Bloch transform, we have:

$$\sigma(H) = \bigcup_{k \in [0, \frac{2\pi}{a}]} \sigma(H_k)$$

where $\sigma(H_k)$ is the spectrum of the operator H restricted on the domain $H^2([0, a])$ with the generalized periodic boundaries conditions:

$$\begin{cases} u(a) = e^{ika} u(0) \\ u'(a) = e^{ika} u'(0) \end{cases}$$

In physics, the interval $[0, \frac{2\pi}{a}]$ for the parameter k is called the Brillouin zone.

Remark 2

Two physicist-style proofs of this theorem in 3D are presented in (2), and a rigorous mathematical proof for the 1D case is developed in (1). To understand where this result comes from, see appendix A.

2.2 How to obtain $\sigma(H_k)$?

The idea is to obtain periodic boundary conditions.

We set $u = e^{ikx} v$. Then we have:

$$\begin{aligned} H_k u &= -\frac{d}{dx^2} u + V(x)u \\ &= e^{ikx} \left[\left(-\frac{d}{dx^2} + 2ik \frac{d}{dx} - k^2 \right) + V(x) \right] v \\ &= e^{ikx} H_{(k)} v \end{aligned}$$

where we introduced the operator $H_{(k)} = \left(-\frac{d}{dx^2} + 2ik \frac{d}{dx} - k^2 \right) + V(x)$.

So we get that $\sigma(H_k)$ is equal to $\sigma(H_{(k)})$ with periodic boundaries conditions.

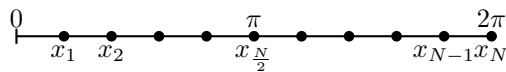
$$\begin{cases} H_k u = \lambda u \\ u(a) = e^{ika} u(0) \\ u'(a) = e^{ika} u'(0) \end{cases} \iff \begin{cases} H_{(k)} v = \lambda v \\ v(a) = v(0) \\ v'(a) = v'(0) \end{cases}$$

We need to compute the spectrum of $H_{(k)}$. This operator contains the derivative and the second derivative. They are of infinite dimension, but we need finite dimension operators to calculate numerically the eigenvalues.

Differentiation Matrices

To work with finite dimension, we approximate the function v by a vector containing its values on a set of N regularly spaced points over one period. The derivative and second derivative operators are now matrices of size N by N . There are different possible choices for such matrices.

Let's take the period a equal to 2π so that k varies between 0 and 1. The distance between two points is $h = \frac{2\pi}{N}$. We note $v_j := v(x_j)$.



Finite Differentiation

A first approximation of the derivative can be obtained by using finite differentiation. The n -order finite differentiation is given by the derivative of the local polynomial interpolant of degree $\leq n$ (n is even).

More precisely, for the point x_j , the n -order polynomial interpolant of v will be the only polynomial of degree $\leq n$ with

$$p(x_{j+l}) = v_{j+l} \quad \forall l \in \{0, 1, \dots, \frac{N}{2}\}$$

We set $(\mathbf{D}v)_j = p'(x_j)$.

For the second-order, we obtain: $(\mathbf{D}v)_j = \frac{v_{j+1} - v_{j-1}}{2h}$.
Thus, the second-order finite differentiation matrix is tridiagonal circulant:

$$\mathbf{D} = h^{-1} \begin{pmatrix} 0 & \frac{1}{2} & 0 & \cdots & 0 & -\frac{1}{2} \\ -\frac{1}{2} & 0 & \frac{1}{2} & \cdots & 0 & 0 \\ 0 & -\frac{1}{2} & 0 & \ddots & \vdots & \vdots \\ \vdots & \ddots & \ddots & \ddots & \frac{1}{2} & 0 \\ 0 & \cdots & 0 & -\frac{1}{2} & 0 & \frac{1}{2} \\ \frac{1}{2} & 0 & \cdots & 0 & -\frac{1}{2} & 0 \end{pmatrix}$$

For the n -order, the matrix will be $(\frac{n}{2} + 1)$ -diagonal circulant. The accuracy of this method is $O(h^n)$. However, when n increases, the matrix loses its sparse property and it is much longer to calculate its eigenvalues. Numerically, it is more interesting to keep a low order ($n = 4$ is sufficient) and to increase N i.e. reduce h .

Spectral Differentiation

Another way to differentiate v is to use the DFT (Discrete Fourier transform):

$$\hat{v}_k = h \sum_{j=1}^N e^{-ikx_j} v_j$$

Remark 3

Because of the periodicity of v , we have $v_{j+N} = v_j$.

The DFT maintains this property: $\hat{v}_{k+N} = \hat{v}_k$. Moreover, if v is real: $\hat{v}_{-k} = \hat{v}_k^*$.

We now define a trigonometric interpolant with degree at most $\frac{N}{2}$ by:

$$\tilde{p}(x) = \frac{1}{2\pi} \sum_{k=-\frac{N}{2}}^{\frac{N}{2}} e^{ikx} \hat{v}_k$$

where the tilde indicates that the terms $k = \pm \frac{N}{2}$ are multiplied by $\frac{1}{2}$.

\tilde{p} is a linear combination of $1, \cos(x), \sin(x), \cos(2x), \sin(2x), \dots, \cos(\frac{N}{2}x)$ that satisfies $p(x_l) = v_l$.

Proof. The term $\sin(\frac{N}{2}x)$ is not needed since $\hat{v}_{-\frac{N}{2}} = \hat{v}_{\frac{N}{2}}$.

$$\begin{aligned} \tilde{p}(x_l) &= \frac{1}{2\pi} \sum_{k=-\frac{N}{2}}^{\frac{N}{2}} e^{-ikx_l} \hat{v}_k \\ &= \frac{1}{2\pi} \left(\frac{1}{2} \sum_{k=-\frac{N}{2}}^{\frac{N}{2}-1} e^{ikx_l} \hat{v}_k + \frac{1}{2} \sum_{k=-\frac{N}{2}+1}^{\frac{N}{2}} e^{ikx_l} \hat{v}_k \right) \\ &= \frac{h}{2\pi} \sum_{j=1}^N \left(\frac{1}{2} \sum_{k=-\frac{N}{2}}^{\frac{N}{2}-1} e^{ik(x_l-x_j)} v_j + \frac{1}{2} \sum_{k=-\frac{N}{2}+1}^{\frac{N}{2}} e^{ik(x_l-x_j)} v_j \right) \end{aligned}$$

$$\text{If } j \neq l, \quad \sum_{k=-\frac{N}{2}}^{\frac{N}{2}-1} e^{ik(x_l-x_j)} = \frac{e^{-i\frac{N}{2}(x_l-x_j)} - e^{i\frac{N}{2}(x_l-x_j)}}{1 - e^{i(x_l-x_j)}} = \frac{-2i \sin\left(\frac{N}{2}(x_l-x_j)\right)}{1 - e^{i(x_l-x_j)}} = 0$$

$$\sum_{k=-\frac{N}{2}+1}^{\frac{N}{2}} e^{ik(x_l-x_j)} = e^{i(x_l-x_j)} \frac{-2i \sin\left(\frac{N}{2}(x_l-x_j)\right)}{1 - e^{i(x_l-x_j)}} = 0$$

given that $\frac{N}{2}(x_l - x_j) = (l - j)\pi$

$$\text{If } j = l, \quad \sum_{k=-\frac{N}{2}}^{\frac{N}{2}-1} e^{ik(x_l-x_j)} = \sum_{k=-\frac{N}{2}+1}^{\frac{N}{2}} e^{ik(x_l-x_j)} = N$$

So $\tilde{p}(x_l) = \frac{h}{2\pi} N v_l = v_l$.

□

Remark 4

$\frac{1}{2\pi} \sum_{k=-\frac{N}{2}+1}^{\frac{N}{2}} e^{-ikx} \hat{v}_k$ would also work but the interpolant \tilde{p} has the advantage of being real when v is real. Indeed, in this case:

- $\hat{v}_0 = h \sum_{j=1}^N v_j$ is real.
- $\forall k \in [1, \frac{N}{2}], e^{ikx} \hat{v}_k + e^{-ikx} \hat{v}_{-k} = (e^{ikx} \hat{v}_k) + (e^{ikx} \hat{v}_k)^* = 2 \Re(e^{ikx} \hat{v}_k)$

As in the finite differentiation, we are going to set: $(\tilde{\mathbf{D}}v)_j = \tilde{p}'(x_j)$.

The key property for obtaining the spectral differentiation matrix is:

$$\tilde{p}(x) = \sum_{m=1}^N v_m S_N(x - x_m) \text{ with the periodic sinc function } S_N(x) = \frac{\sin(\frac{N}{2}x)}{N \tan(\frac{x}{2})}$$

Proof. Let's write the discretized function v as a linear combination of translated periodic delta function δ . $v_j = \sum_{m=1}^N v_m \delta(x_j - x_m)$

$$\delta_j := \delta(x_j) = \begin{cases} 1 & \text{if } j \equiv 0 \pmod{N} \\ 0 & \text{if } j \not\equiv 0 \pmod{N} \end{cases}$$

By the linearity of the interpolation, we have: $\tilde{p}(x) = \sum_{m=1}^N v_m \tilde{p}_\delta(x - x_m)$

Now, $\hat{\delta}_j = h$ for each j so the trigonometric interpolant for δ is:

$$\begin{aligned} \tilde{p}_\delta(x) &= \frac{h}{2\pi} \sum_{k=-\frac{N}{2}}^{\frac{N}{2}} e^{ikx} = \frac{h}{2\pi} \left(\frac{1}{2} \sum_{k=-\frac{N}{2}}^{\frac{N}{2}-1} e^{ikx} + \frac{1}{2} \sum_{k=-\frac{N}{2}+1}^{\frac{N}{2}} e^{ikx} \right) \\ &= \frac{h}{2\pi} \frac{1 + e^{ix}}{1 - e^{ix}} \left(-i \sin\left(\frac{N}{2}x\right) \right) \text{ (see the previous proof)} \\ &= \frac{h}{2\pi} \frac{\cos(\frac{x}{2})}{\sin(\frac{x}{2})} \sin\left(\frac{N}{2}x\right) = S_N(x) \end{aligned}$$

□

From $\tilde{p}'(x_j) = \sum_{m=1}^N v_m S'_N(x_j - x_m)$, we deduce: $\tilde{\mathbf{D}}_{jm} = S'_N(x_j - x_m)$.

Given the derivative of the periodic sinc function:

$$S'_N(x_j) = \begin{cases} 0 & \text{if } j \equiv 0 \pmod{N} \\ \frac{1}{2}(-1)^j \cot(jh/2) & \text{if } j \not\equiv 0 \pmod{N} \end{cases}$$

we get the spectral differentiation matrix:

$$\tilde{\mathbf{D}} = \begin{pmatrix} 0 & \frac{1}{2} \cot(\frac{1h}{2}) & -\frac{1}{2} \cot(\frac{2h}{2}) & \cdots & \cdots & \frac{1}{2} \cot(\frac{(N-1)h}{2}) \\ -\frac{1}{2} \cot(\frac{1h}{2}) & 0 & \frac{1}{2} \cot(\frac{1h}{2}) & & & \vdots \\ \frac{1}{2} \cot(\frac{2h}{2}) & -\frac{1}{2} \cot(\frac{1h}{2}) & 0 & \ddots & & \vdots \\ \vdots & & \ddots & \ddots & \frac{1}{2} \cot(\frac{1h}{2}) & \frac{1}{2} \cot(\frac{2h}{2}) \\ \vdots & & & & -\frac{1}{2} \cot(\frac{1h}{2}) & 0 \\ -\frac{1}{2} \cot(\frac{(N-1)h}{2}) & \cdots & \cdots & \frac{1}{2} \cot(\frac{2h}{2}) & -\frac{1}{2} \cot(\frac{1h}{2}) & -\frac{1}{2} \cot(\frac{1h}{2}) \end{pmatrix}$$

By further differentiation of S_N we can construct the differentiation matrix of any order. I used the spectral differentiation matrices of first $\tilde{\mathbf{D}}$ and second-order $\tilde{\mathbf{D}}^{(2)}$. I want to mention here L. N. Trefethen's excellent pedagogical work (3), where the differentiation matrices are very well explained, and which offers a simple and compact MATLAB implementation of $\tilde{\mathbf{D}}$ and $\tilde{\mathbf{D}}^{(2)}$ that served as the starting point for my codes.

Why is the spectral method more efficient?

Even though the spectral differentiation matrices are not sparse, the convergence of their eigenvalue is much faster than with the finite differentiation matrices. This is because the convergence rate is $O(N^{-m})$ for every m for functions that are smooth and even $O(c^N)$ ($0 < c < 1$) for functions that are analytic, which is often the case of the eigenfunctions.

A proof of this convergence rate is provided in (3). It is based on the relationship between the function's smoothness and its Fourier transform's decay. As a reminder, if $u \in L^2(\mathbb{R})$ has p continuous derivatives in $L^2(\mathbb{R})$, then $\hat{u}(k) = O(|k|^{-(p+1)})$ as $k \rightarrow \infty$.

We approximate $H_{(k)} = \left(-\frac{d}{dx^2} + 2ik\frac{d}{dx} + k^2 \right) + V(x)$ by $(-\tilde{\mathbf{D}}^{(2)} + 2ik\tilde{\mathbf{D}} + k^2\mathbf{I}) + \mathbf{V}$
where \mathbf{I} is the identity of size N by and \mathbf{V} the diagonal matrix with $V_{jj} = V(x_j)$.

Remark 5

For all $k \in [0, 1]$, $\sigma(H_{(k)})$ is an infinite discrete set $\{\lambda_1(k), \lambda_2(k), \lambda_3(k)\dots\}$ To calculate the eigenvalues of $H_{(k)}$ I used the MATLAB routines `eigs(Hk, Neig, 'smallestabs')` or `eigs(Hk, Neig, 'smallestreal')`, depending on whether I wanted to calculate the first $Neig$ eigenvalues of H_k by increasing real part or modulus. In the non-selfadjoint case, it is not equivalent.

2.3 First experiments

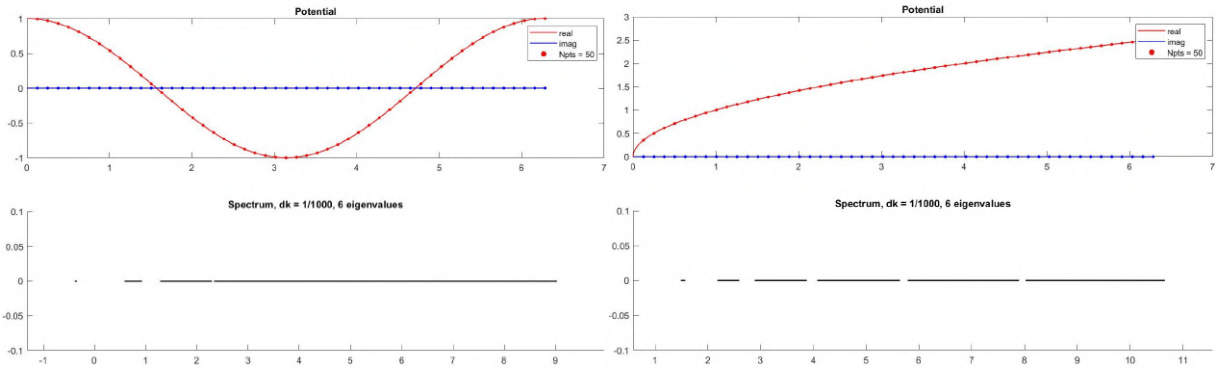
$$\sigma(H) = \bigcup_{k \in [0, 1]} \sigma(H_{(k)}) \quad \text{given our choice of } a = 2\pi$$

Numerically we can only calculate $\sigma(H_{(k)})$ for a finite number of values of k . Let's take a regular subdivision of the interval 0 to 1.

2 FIRST STEPS IN 1D

V real

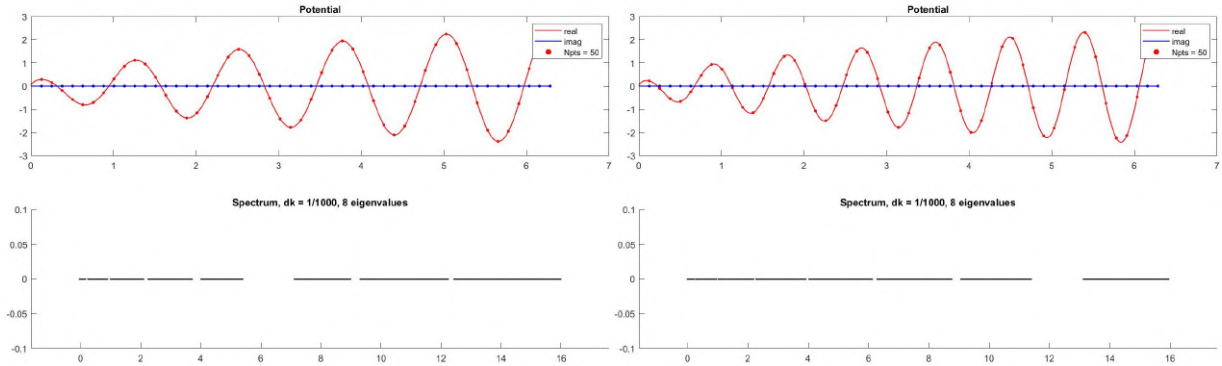
Let's have a look at the results for 1000 values of k and $N = 50$. A band spectrum is observed. The n th band corresponds to the set of values covered by $\lambda_n(k)$ as k varies between 0 and 1. One can observe properties presented in the work (4) by Peter Kuchment.



$$V(x) = \cos(x)$$

$$V(x) = \sqrt{x}$$

The rate of the gaps' sizes decay when $n \rightarrow \infty$ determines the smoothness of the potential. For instance, C^∞ potentials correspond to the gap size decaying faster than any power of $\frac{1}{n}$. Indeed, for $V(x) = \cos(x)$ we can't see the spacing between the 4th and 5th eigenvalues, as well as between the 5th and 6th, is no longer visible. For $V(x) = \sqrt{x}$, the gap size decay is much slower (in this case, the potential is not even continuous).



$$V(x) = \sqrt{x} \cos(5x)$$

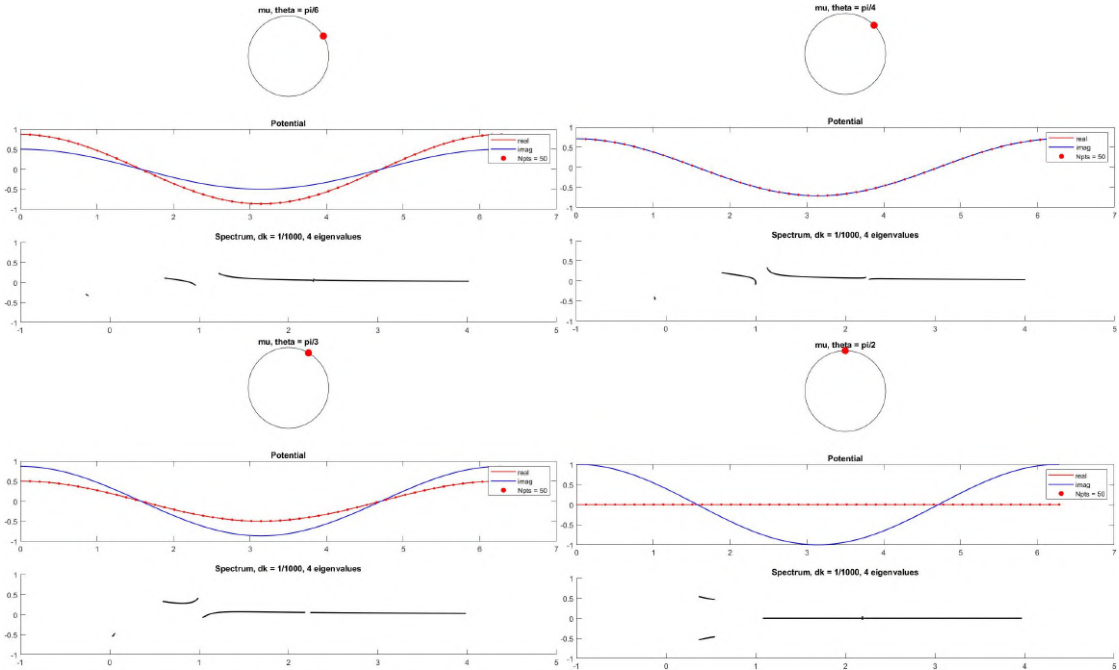
$$V(x) = \sqrt{x} \cos(7x)$$

With some potentials, we can have spectral gap that start to increase before to decrease as expected. If we take $V(x) = \sqrt{x} \cos(px)$, the size of the p first gap is increasing then decreasing.

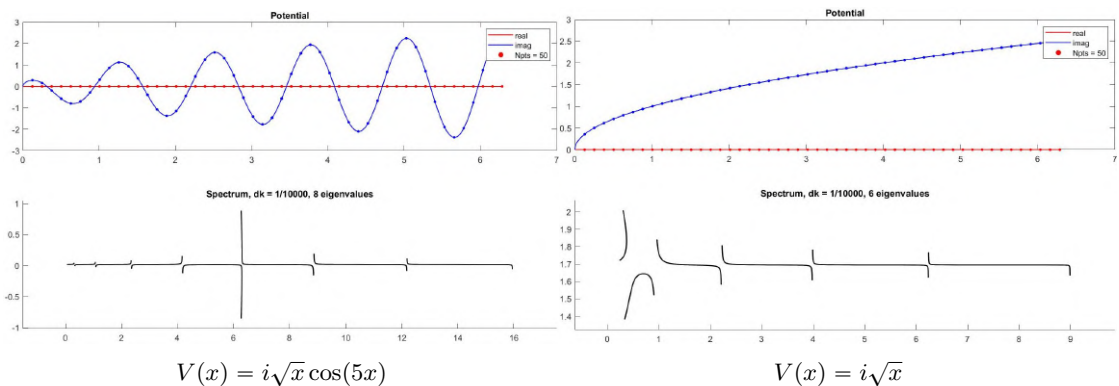
2 FIRST STEPS IN 1D

V complex

If the potential is complex, the spectrum is no longer confined to the real axis. However, it still takes the form of bands. An experiment I made was to see how the spectrum evolves when we take $V(x) = \mu \cos(x)$ with $\mu = e^{i\theta}$ with moving along the unit circle.



We can notice that between $\theta = \pi/4$ and $\theta = \pi/3$, bands 2 and 3 change convexity without crossing. Just below what we get when we multiply previously used potentials by i .



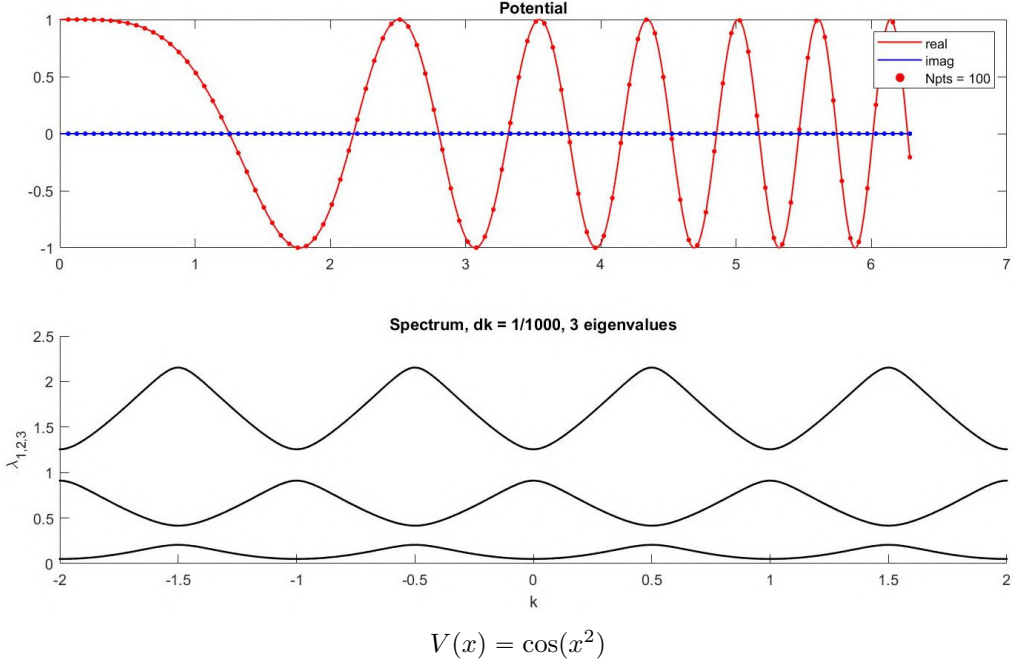
Again, each band corresponds to the set of values covered by a certain $\lambda_n(k)$ as k varies in the whole Brillouin zone $\mathcal{B}_{1D} = [0, 1]$.

2 FIRST STEPS IN 1D

$\lambda_n(k)$ as a function of k

In the selfadjoint case, numbering $\sigma(H_k)$ is trivial as it is a discrete set of \mathbb{R} that we can index by increasing order: $\lambda_1(k) \leq \lambda_2(k) \leq \lambda_3(k) \leq \dots$

For each n , if we plot $\lambda_n(k)$ as a function of k , a continuous function is obtained.



We notice here 2 things :

- (i) The $\lambda_n(k)$ function are 1-periodic.
- (ii) The λ_n functions are even.

Floquet-Bloch theorem gives us: $\sigma(H) = \bigcup_{k \in [0, \frac{2\pi}{a}]} \sigma(H_k)$

If we look at the generalized boundaries conditions for H_k , it is immediately clear that:

$$\sigma(H_k) = \sigma(H_{k+n\frac{2\pi}{a}}) \quad \forall n \in \mathbb{Z} \quad (*)$$

which explains (i) given that $a = 2\pi$ in our codes.

Moreover we have:

$$\begin{aligned} \sigma(H) &= \bigcup_{k \in [0, \frac{\pi}{a}]} \sigma(H_k) + \bigcup_{k \in [\frac{\pi}{a}, \frac{2\pi}{a}]} \sigma(H_k) \\ &= \bigcup_{k \in [0, \frac{\pi}{a}]} \sigma(H_k) + \bigcup_{k \in [-\frac{\pi}{a}, 0]} \sigma(H_k) \quad \text{by (*) with } n = -1 \\ &= \bigcup_{k \in [0, \frac{\pi}{a}]} \sigma(H_k) \cup \sigma(H_{-k}) \end{aligned}$$

3 FIRST STEPS IN 2D

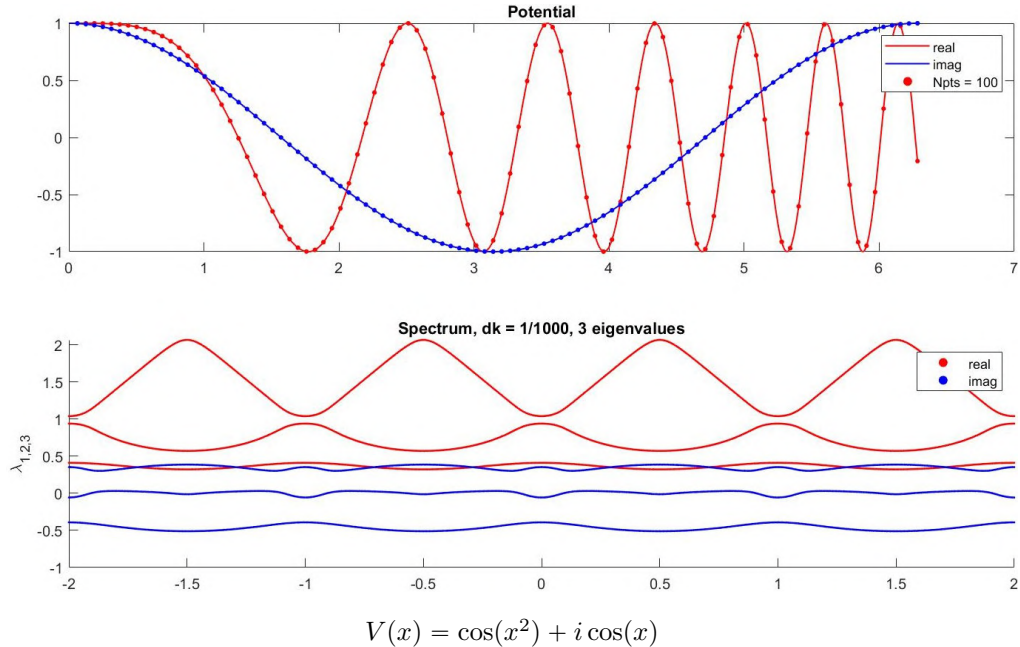
Using the Hill discriminant Δ (see appendix A), presented in detail in (1) and whose properties are summarized in (4), we observe that: $\lambda \in \sigma(H_k) \iff \Delta(\lambda) - 2 \cos(ka) = 0$. Given the parity of the cosine function, we get: $\sigma(H_k) = \sigma(H_{-k})$ which explains (ii) and allows us to write:

$$\sigma(H) = \bigcup_{k \in [0, \frac{\pi}{a}]} \sigma(H_k)$$

Only half of the Brillouin zone is needed to get the full spectrum! In our code, we only need to vary k between 0 and 0.5. If we look at the movement of λ as a function of k , we can see that it starts from one end of the band at $k = 0$, reaches the other end at $k = 0.5$, then turns around and returns to the starting end at $k = 1$.

Remark 6

In (1) and (4), the Hill discriminant is introduced for a real V but we can see that it could be done for a complex V . If we plot $\Re(\lambda_n(k))$ and $\Im(\lambda_n(k))$, we observe the same properties.



3 First steps in 2D

In \mathbb{R}^2 , our operator is:

$$H = -\Delta + V(x_1, x_2) = -\frac{d}{dx_1^2} - \frac{d}{dx_2^2} + V(x_1, x_2)$$

where $V : \mathbb{R}^2 \rightarrow \mathbb{C}$ is bounded and satisfies:

$$V(x_1, x_2) = V(x_1 + na, x_2 + mb) \quad \forall n, m \in \mathbb{Z}$$

In other words,

$\forall x_2 \in \mathbb{R}, V(\cdot, x_2)$ is bounded and a -periodic
 $\forall x_1 \in \mathbb{R}, V(x_1, \cdot)$ is bounded and b -periodic.

Thus, the domain of our operator H is the Sobolev space $H^2(\mathbb{R}^2)$.

3.1 Floquet-Bloch transform

The formulation of the Floquet-Bloch transform in 2D is:

$$\sigma(H) = \bigcup_{(k_1, k_2) \in [0, \frac{2\pi}{a}] \times [0, \frac{2\pi}{b}]} \sigma(H_{k_1, k_2})$$

where $\sigma(H_{k_1, k_2})$ is the spectrum of the operator H restricted on $H^2([0, a] \times [0, b])$ with the generalized periodic boundary conditions:

$$\begin{cases} u(a, x_2) = e^{ika} u(0, x_2) & \forall x_2 \in [0, b] \\ u(x_1, b) = e^{ikb} u(x_1, 0) & \forall x_1 \in [0, a] \\ u'(a, x_2) = e^{ika} u'(0, x_2) & \forall x_2 \in [0, b] \\ u'(x_1, b) = e^{ikb} u'(x_1, 0) & \forall x_1 \in [0, a] \end{cases}$$

3.2 How to obtain $\sigma(H_{k_1, k_2})$?

Again we want to obtain periodic boundary conditions.

We set $u = e^{i(k_1 x_1 + k_2 x_2)} v$. Then we have:

$$\begin{aligned} H_{k_1, k_2} u &= -\frac{d}{dx_1^2} u - \frac{d}{dx_2^2} u + V(x_1, x_2) u \\ &= e^{i(k_1 x_1 + k_2 x_2)} \left[-\left(\frac{d}{dx_1^2} + 2ik_1 \frac{d}{dx_1} - k_1^2 \right) - \left(\frac{d}{dx_2^2} + 2ik_2 \frac{d}{dx_2} - k_2^2 \right) + V(x_1, x_2) \right] v \\ &= e^{ikx} H_{(k_1, k_2)} v \end{aligned}$$

where we introduced the operator

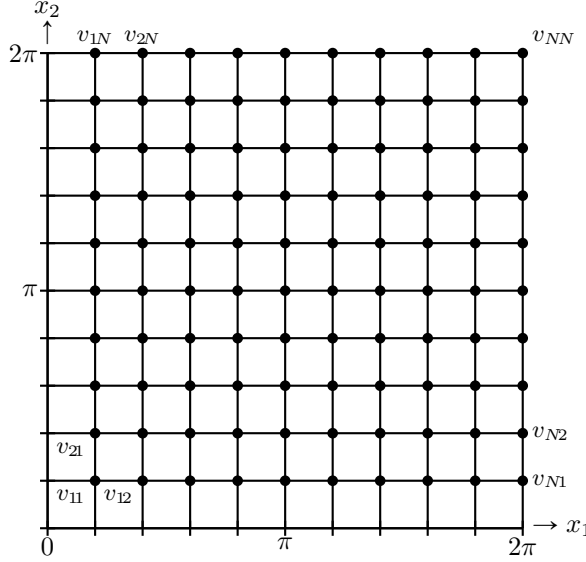
$$H_{(k_1, k_2)} = -\left(\frac{d}{dx_1^2} + 2ik_1 \frac{d}{dx_1} - k_1^2 \right) - \left(\frac{d}{dx_2^2} + 2ik_2 \frac{d}{dx_2} - k_2^2 \right) + V(x_1, x_2)$$

So we get that $\sigma(H_{k_1, k_2})$ is equal to $\sigma(H_{(k_1, k_2)})$ with periodic boundaries conditions.

$$\begin{cases} H_{k_1, k_2} u = \lambda u \\ u(a, \cdot) = e^{ika} u(0, \cdot) \\ u(\cdot, b) = e^{ikb} u(\cdot, 0) \\ u'(a, \cdot) = e^{ika} u'(0, \cdot) \\ u'(\cdot, b) = e^{ikb} u'(\cdot, 0) \end{cases} \iff \begin{cases} H_{(k_1, k_2)} v = \lambda v \\ v(a, \cdot) = v(0, \cdot) \\ v(\cdot, b) = v(\cdot, 0) \\ v'(a, \cdot) = v'(0, \cdot) \\ v'(\cdot, b) = v'(\cdot, 0) \end{cases}$$

3 FIRST STEPS IN 2D

To work with finite dimension, we approximate a function $v \in H^2([0, a] \times [0, b])$ by a vector containing its values on a grid of $N_1 \times N_2$ regularly spaced points over $[0, a] \times [0, b]$. Let's take $a = b = 2\pi$ and $N_1 = N_2$.



We note $v_{ij} := v(x_i, x_j)$ and arrange the different values in a vector v^\rightarrow of length N^2 with the following order:

$$v^\rightarrow = \begin{pmatrix} w_1^\rightarrow \\ w_2^\rightarrow \\ \vdots \\ w_N^\rightarrow \end{pmatrix} \quad \text{where} \quad w_i^\rightarrow = \begin{pmatrix} v_{i1} \\ v_{i2} \\ \vdots \\ v_{iN} \end{pmatrix}$$

It is immediate that the first derivative and second derivative with regard to x_1 are (using the spectral differentiation matrix $\tilde{\mathbf{D}}$ and $\tilde{\mathbf{D}}^{(2)}$ of size N for the 1D case):

$$\frac{\partial}{\partial x_1} v^\rightarrow = \begin{pmatrix} \tilde{\mathbf{D}} w_1^\rightarrow \\ \tilde{\mathbf{D}} w_2^\rightarrow \\ \vdots \\ \tilde{\mathbf{D}} w_N^\rightarrow \end{pmatrix} = \begin{pmatrix} \tilde{\mathbf{D}} & & & \\ & \tilde{\mathbf{D}} & & \\ & & \ddots & \\ & & & \tilde{\mathbf{D}} \end{pmatrix} \begin{pmatrix} w_1^\rightarrow \\ w_2^\rightarrow \\ \vdots \\ w_N^\rightarrow \end{pmatrix} = (\mathbf{I} \otimes \tilde{\mathbf{D}}) v^\rightarrow$$

$$\frac{\partial^2}{\partial x_1^2} v^\rightarrow = \begin{pmatrix} \tilde{\mathbf{D}}^{(2)} w_1^\rightarrow \\ \tilde{\mathbf{D}}^{(2)} w_2^\rightarrow \\ \vdots \\ \tilde{\mathbf{D}}^{(2)} w_N^\rightarrow \end{pmatrix} = \begin{pmatrix} \tilde{\mathbf{D}}^{(2)} & & & \\ & \tilde{\mathbf{D}}^{(2)} & & \\ & & \ddots & \\ & & & \tilde{\mathbf{D}}^{(2)} \end{pmatrix} \begin{pmatrix} w_1^\rightarrow \\ w_2^\rightarrow \\ \vdots \\ w_N^\rightarrow \end{pmatrix} = (\mathbf{I} \otimes \tilde{\mathbf{D}}^{(2)}) v^\rightarrow$$

We can show that the first derivative and second derivative with regard to x_2 are:

$$\frac{\partial}{\partial x_2} = \tilde{\mathbf{D}} \otimes \mathbf{I} \quad \text{and} \quad \frac{\partial^2}{\partial x_2^2} = \tilde{\mathbf{D}}^{(2)} \otimes \mathbf{I}$$

(see appendix B)

$$H_{(k_1, k_2)} = -\left(\frac{d}{dx_1^2} + 2ik_1 \frac{d}{dx_1} - k_1^2\right) - \left(\frac{d}{dx_2^2} + 2ik_2 \frac{d}{dx_2} - k_2^2\right) + V(x_1, x_2)$$

is approximated by

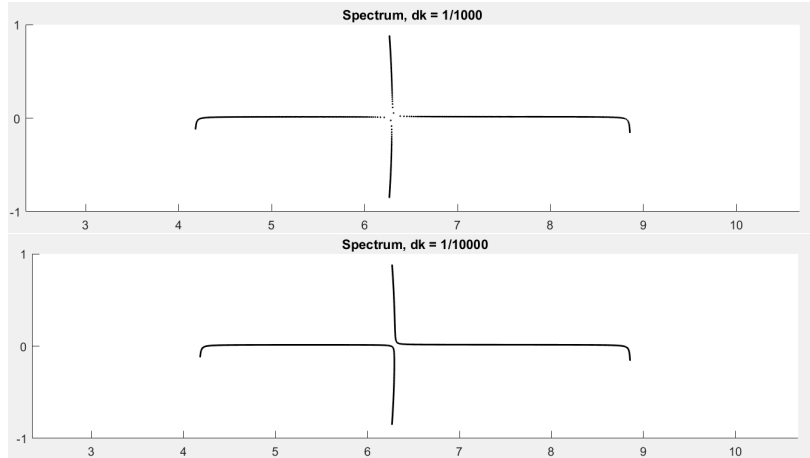
$$-\left(\mathbf{I} \otimes \tilde{\mathbf{D}}^{(2)} + 2ik_1 \mathbf{I} \otimes \tilde{\mathbf{D}} - k_1^2 \mathbf{I}_{N^2}\right) - \left(\tilde{\mathbf{D}}^{(2)} \otimes \mathbf{I} + 2ik_2 \tilde{\mathbf{D}} \otimes \mathbf{I} - k_2^2 \mathbf{I}_{N^2}\right) + \mathbf{V}_{N^2}$$

where \mathbf{I}_{N^2} is the identity of size $N \times N$ and \mathbf{V}_{N^2} the $N \times N$ diagonal matrix which contains all the values $V_{ij} = V(x_i, x_j)$ arranged in the same order as for v .

3.3 First experiments

$$\sigma(H) = \bigcup_{(k_1, k_2) \in [0, 1] \times [0, 1]} \sigma(H_{k_1, k_2})$$

but we can only calculate $\sigma(H_{k_1, k_2})$ for a finite number of pair (k_1, k_2) . The first thing we can try is to take a regular subdivision of $[0, 1] \times [0, 1]$. In the 1D case, with 1000 values of k and $N = 50$, the calculation takes less than 2 seconds. Sometimes 1000 values of k were not enough to achieve a smooth visual appearance, but we could use 10000 values, and the computation time remained under 20 seconds.



Zoom on the bands corresponding to $\lambda_5([0, 1])$ and $\lambda_6([0, 1])$ for $V(x) = i\sqrt{x} \cos(5x)$

In two dimensions, it is not possible to get this smooth visual appearance in less than hours by using the discretization method. Indeed, if we take the same spacing, then we have 1000×1000 values for (k_1, k_2) . If the matrices were of same size than in the 1D case, this would lead to a calculation time of 1000×2 seconds ≈ 0.5 hour. But the size of the matrices is now N^2 so it is much longer to calculate their eigenvalues.

However, there are a few things we can do to reduce the computation time:

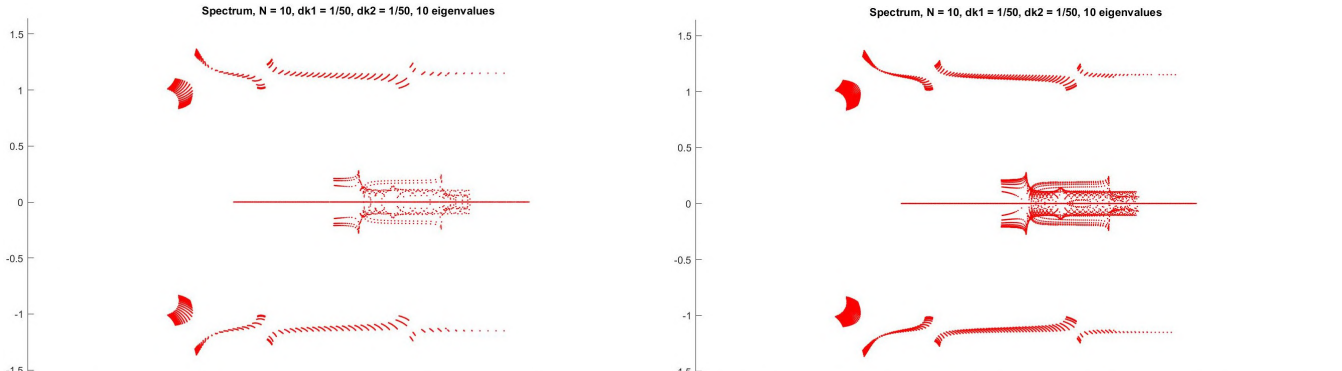
- Taking $N = 10$ is sufficient.
This allows us to work with matrices of size 100, so only 2 times bigger than in 1D.

3 FIRST STEPS IN 2D

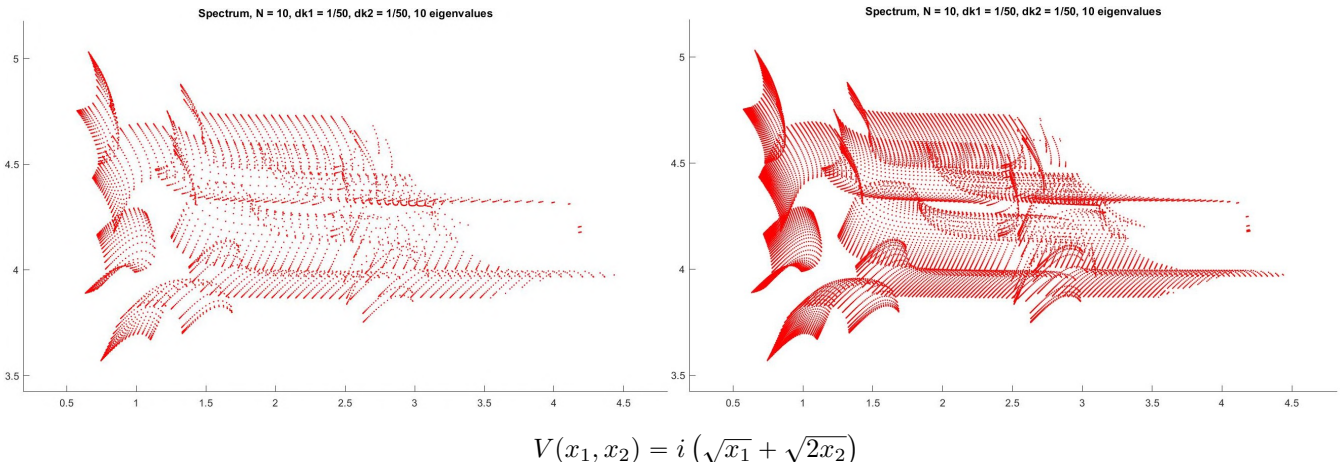
- Reducing the Brillouin zone.

We have already seen in 1D that one half of the Brillouin zone is enough to get the spectrum. In the 2D case, it seems that we can use the quarter $[0, \frac{\pi}{a}] \times [0, \frac{\pi}{b}]$ instead of $[0, \frac{2\pi}{a}] \times [0, \frac{2\pi}{b}]$. We were able to prove this in the case where $V(x_1, x_2) = V_1(x_1) + V_2(x_2)$. (see appendix C)

Below the pictures we get with (k_1, k_2) in a 50×50 grid of $[0, 1]^2$ then $[0, 0.5]^2$.

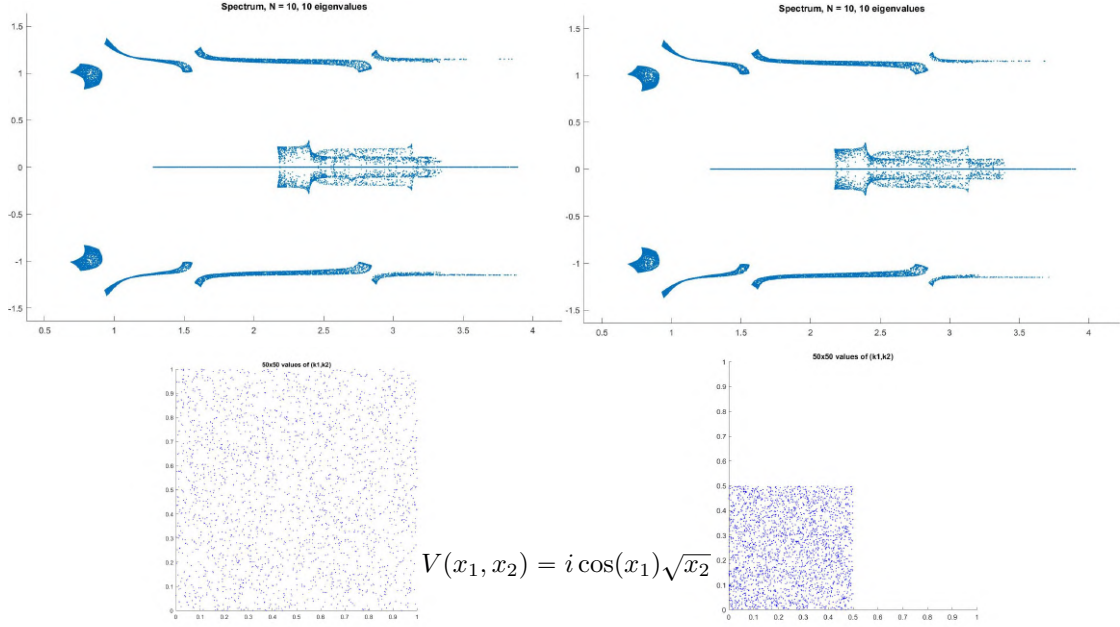


All the pictures require the same computational time (around 14 seconds) but the right ones are much more refined. In the 50×50 grid of $[0, 1]^2$, some pairs of (k_1, k_2) were equivalent.

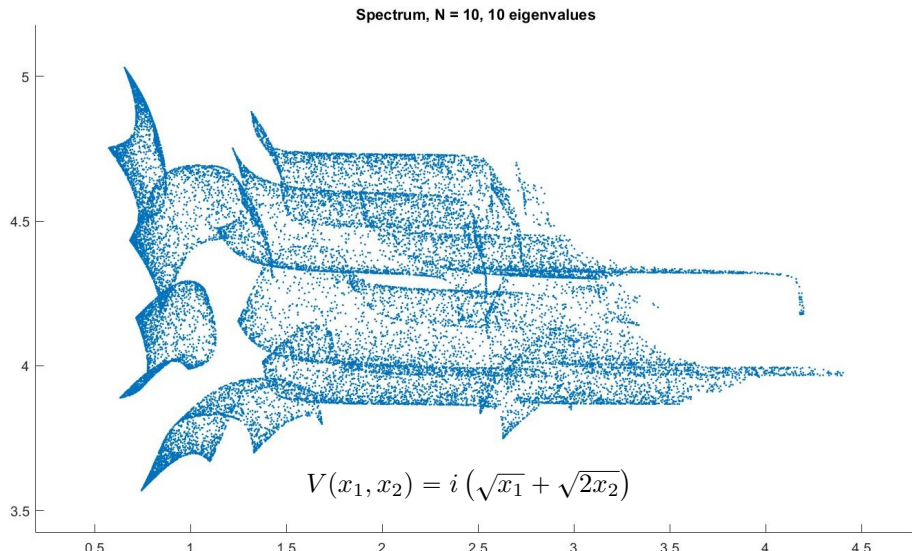


Using a regular subdivision leads to the appearance of lines that disrupt the continuity of the connected components of the spectrum. What happens if we take random values of (k_1, k_2) ?

3 FIRST STEPS IN 2D



With random values, reducing the Brillouin zone doesn't give us any improvement of the spectrum. Indeed, the random aspect already provides non-equivalent values of (k_1, k_2) in $[0, 1]^2$. However, we notice that some outlines are better defined and that areas that appear empty with the regular method are filled. Moreover, we can visually guess connected components that correspond to the set of values covered by a certain $\lambda_n(k_1, k_2)$ as k varies in the whole Brillouin zone \mathcal{B}_{2D} .

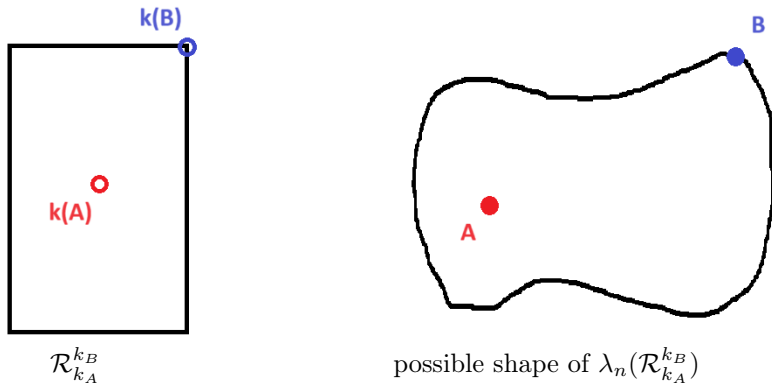


Even though it is already better, we can see areas that are more or less dense. In the third section, we will try to implement various strategies to fill these areas.

4 Some ideas of improvements

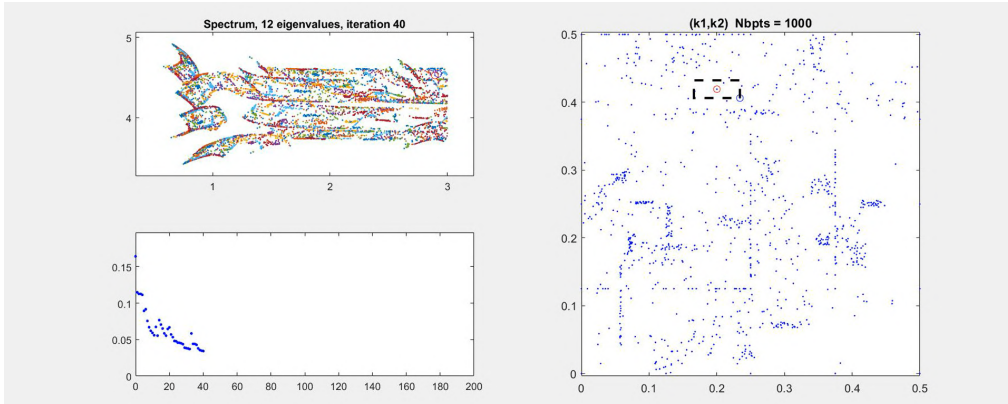
4.1 Finding good values of \mathbf{k}

I tried to improve the random method by picking up $\mathbf{k} = (k_1, k_2)$ in a half-random half-targeted way. It is an iterative process. First, we randomly draw n_k values of k . Then we search for the most isolated point A in the spectrum (the point with the biggest distance to its closest neighbor). At the next iteration, we randomly draw n_k new values of \mathbf{k} in the rectangle $\mathcal{R}_{k_A}^{k_B}$, with center the \mathbf{k}_A corresponding to the isolated point A and corner \mathbf{k}_B corresponding to its closest neighbor B in the spectrum. And so on...



This restricted area for new values of \mathbf{k} was chosen given that the $\lambda_n(\mathbf{k})$ are continuous. We hope that we will get values of $\lambda_n(\mathcal{R}_{k_A}^{k_B})$ that are closer to A than B .

Let's have a look at the evolution with $N_{\text{it}} = 200$ iterations for $V(x_1, x_2) = i(\sqrt{x} + \sqrt{2y})$ and $n_k = 25$. For each value of \mathbf{k} , we search for the N_{eig} first eigenvalues in modulus.

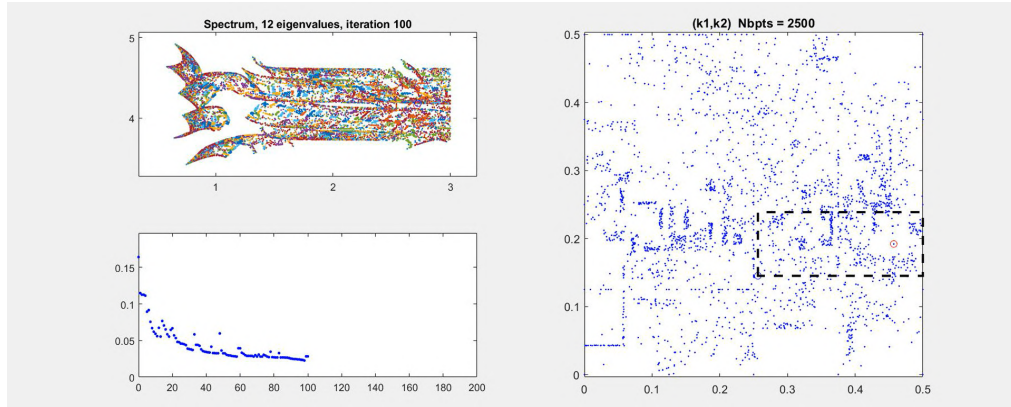


We can see that this way of picking up new $\mathbf{k} = (k_1, k_2)$ is very efficient at the beginning. With only 1000 values of k we already have a good picture of the spectrum. Bottom left is plotted the distance d of the most isolated point to its closest neighbor. d decays very fast for the first iterations. On the right are displayed the random values of k that have been used, as well as the rectangle where the next draw will take place.

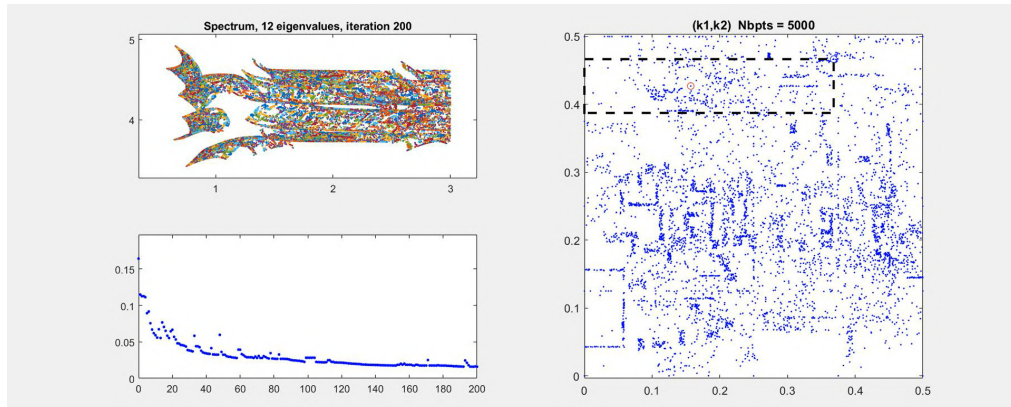
Remark 7

d does not decrease monotonically, because when new values of k are drawn, they can result in new points of the spectrum that are even more isolated.

For comparison, here is what we obtain with $2500 = 50 \times 50$ values of \mathbf{k} , which is the same number of points as on page 18.



After a certain number of iterations, d decreases only very slowly, because the spacing between the points has become homogeneous.



This method presents a lot of problems:

- Computational time:

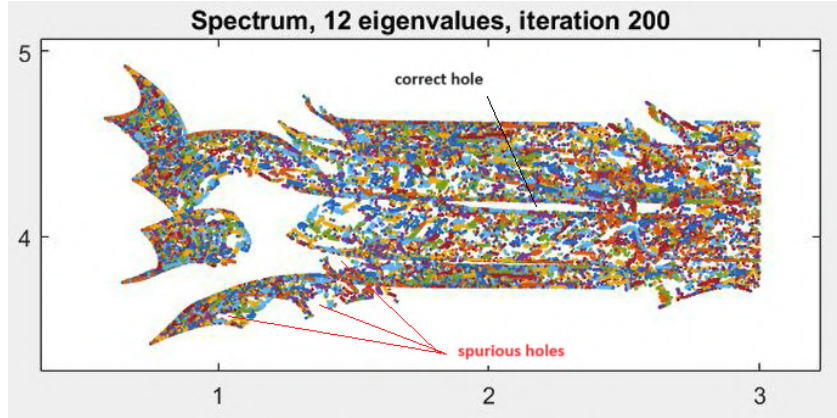
At each iteration, we have to search for the most isolated point on the spectrum which requires evaluating n_s^2 distances, with n_s the actual number of points of the spectrum, which increases of a constant number ($n_k \times N_{\text{eig}}$) at each iteration. The sum of the first n squares of integers is proportional to n^3 , so we get the complexity:

$$\mathcal{O}(n_k^2 N_{\text{eig}}^2 N_{\text{it}}^3)$$

4 SOME IDEAS OF IMPROVEMENTS

- Unexpected holes in the spectrum:

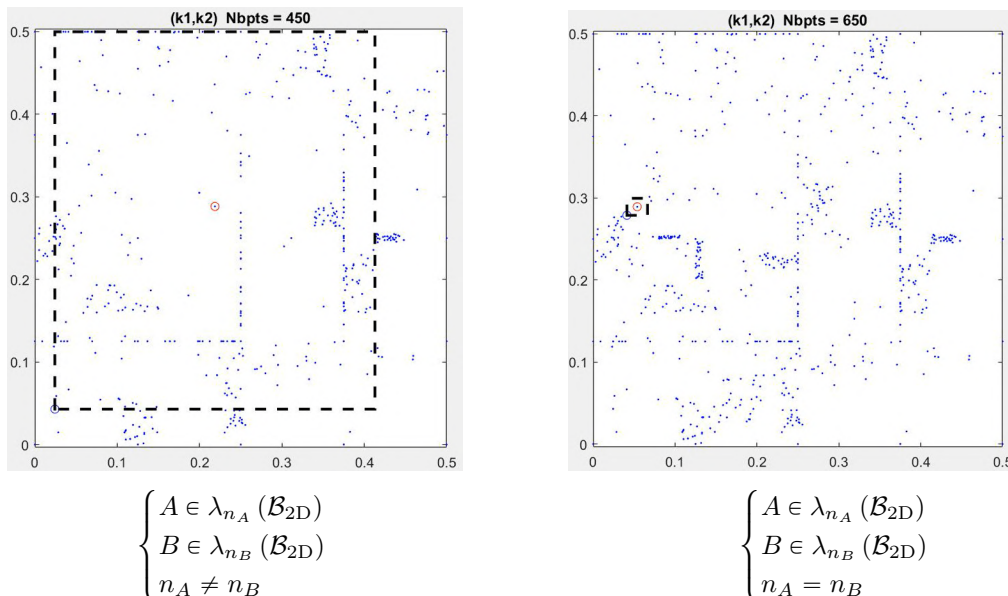
If we compare the spectrum below to the one page 18, we can observe that there are some holes that should be filled.



Why does this happen? If we look at the points around such hole, they are not isolated (they are close to each other) so the probability that new points are going to be added here is very low. It is impossible to know if those holes are artifacts or if $\sigma(H)$ is really empty there...

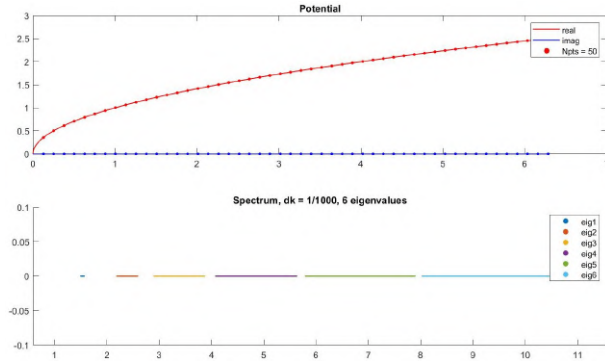
- The $\lambda_n(\mathbf{k})$ functions are not identified:

When we search for the most isolated point A of the spectrum, it is possible and often the case that A and its closest neighbor B are not values from the same $\lambda_n(\mathbf{k})$ function, which explains why the distance between \mathbf{k}_A and \mathbf{k}_B in the Brillouin zone \mathcal{B}_{2D} is sometimes very big.



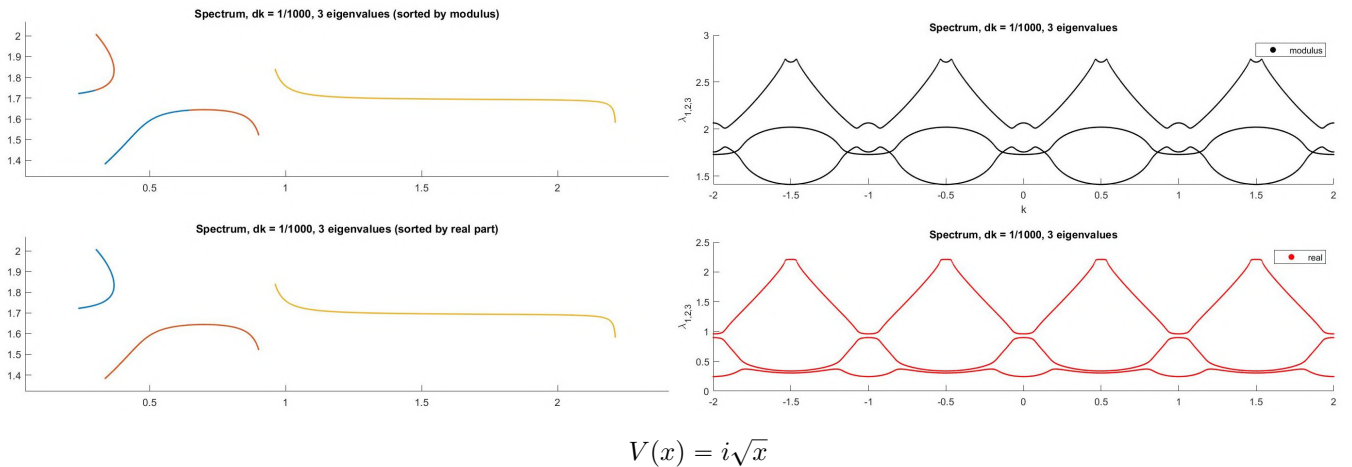
4.2 Identifying the connected components $\lambda_n(\mathcal{B}_{2D})$

In the one-dimensional case with a real-valued potential, if for each value of k , we label the eigenvalues of H_k in ascending order, we can then easily identify the continuous functions $\lambda_n(k)$ by displaying them in different colors.



$$V(x) = \sqrt{x}$$

When V is complex, we must be more careful about how we rank the eigenvalues of H_k for each k . For $V(x) = i\sqrt{x}$, if we rank them by ascending modulus order, there is a mistake because the functions $|\lambda_1(k)|$ and $|\lambda_2(k)|$ intersect each other. We identify correctly the $\lambda_n(k)$ functions if we rank $\sigma(H_k)$ by ascending real part because the $\Re(\lambda_n(k))$ do not intersect each other.

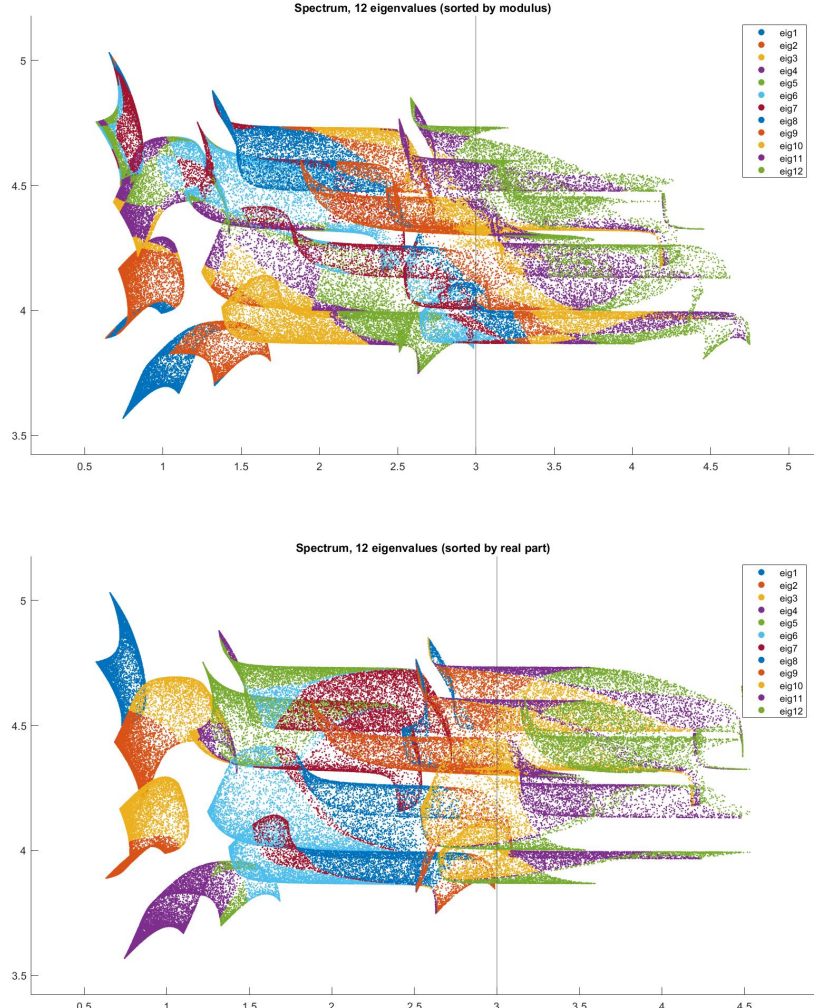


$$V(x) = i\sqrt{x}$$

In the 2D case, there is no simple way to identify the $\lambda_n(k)$ functions...

We could already see p.18 that the connected components $\lambda_n(\mathcal{B}_{2D})$ overlap each other. This is even more visible in the next picture where we draw 100×100 random values of \mathbf{k} .

4 SOME IDEAS OF IMPROVEMENTS



$$V(x_1, x_2) = i (\sqrt{x_1} + \sqrt{2x_2})$$

Except for the top left block, colored and identified as $\lambda_1(\mathcal{B}_{2D})$ by the sorting method based on increasing real part, we can see that these two sorting methods do not work at all in two dimensions.

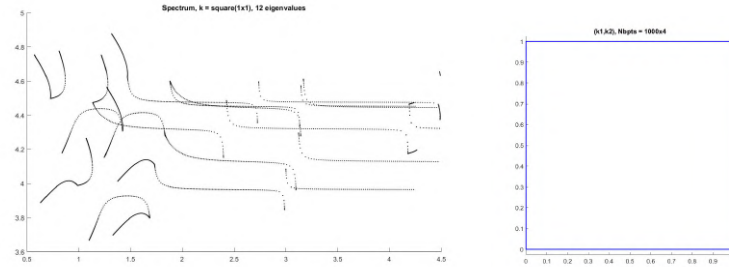
Remark 8

To the right of the vertical line corresponding to $\text{Re}(\lambda) > 3$, the displayed spectrum is not reliable because more eigenvalues would be needed to fill this space.

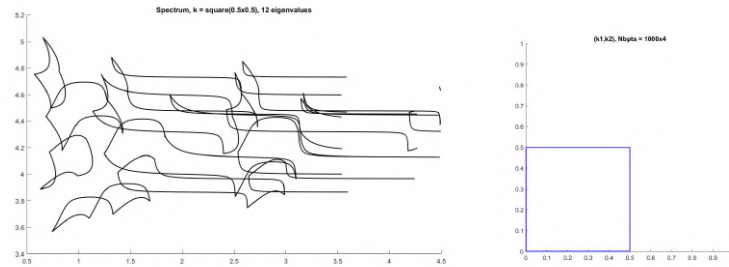
4 SOME IDEAS OF IMPROVEMENTS

The problem with randomly selecting values of \mathbf{k} is that \mathbf{k} does not vary continuously, and therefore, the continuity of the functions λ cannot be exploited to identify them. If \mathbf{k} moves along a continuous path in the Brillouin zone, then the $\lambda_n(\mathbf{k})$ should draw a continuous path in the spectrum.

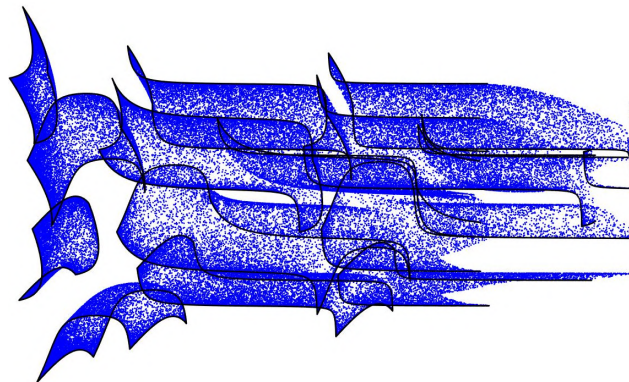
If we move \mathbf{k} along the boundaries of the Brillouin zone, the drawn lines by the $\lambda_n(\mathbf{k})$ functions are:



It is surprising because we don't have closed loops in the spectrum. This is because the opposite edges of the full Brillouin zone \mathcal{B}_{2D} are equivalent. We need to use the boundaries of the quarter $\mathcal{B}_{2D}^{\frac{1}{4}}$ of the Brillouin zone to get closed loops.



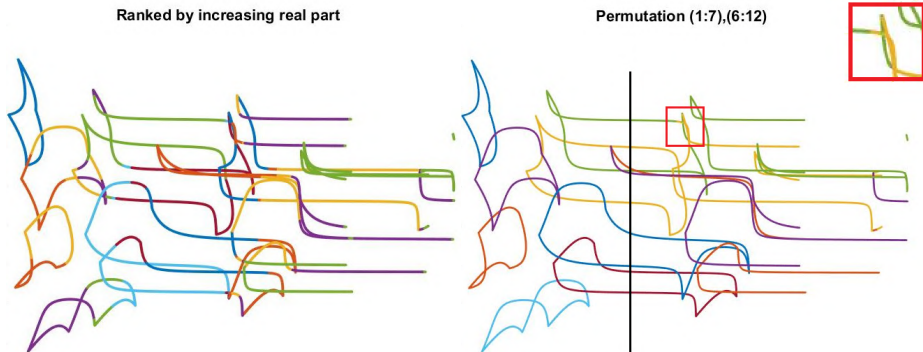
If we add to these black loops points of the spectrum obtained with random values of \mathbf{k} , it seems to fill all the inside.



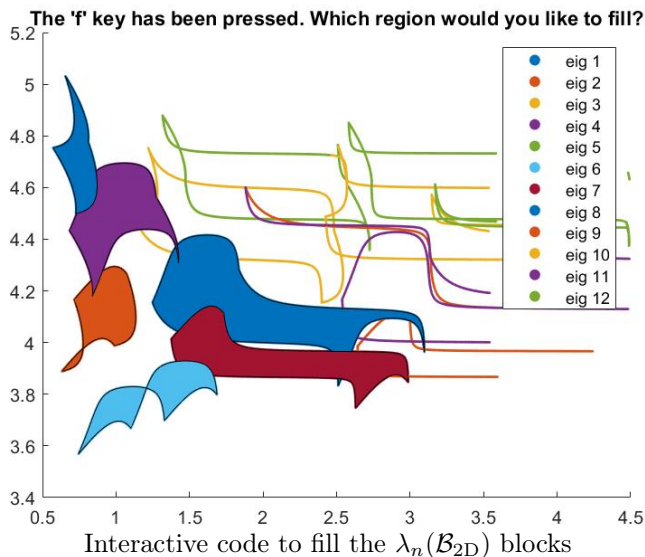
4 SOME IDEAS OF IMPROVEMENTS

Thus, filling these loops with the MATLAB command `fill(xlist,ylist,color)` would be interesting. In order to do it, we need to be able to identify each loop. Moreover the command `fill` need a continuous evolution of `xlist` and `ylist`.

For each value of \mathbf{k} , we get a vector $v_{\mathbf{k}}$ of `Neig` eigenvalues ranked by increasing real part. When \mathbf{k} varies over $\partial\mathcal{B}_{2D}^{\frac{1}{4}}$, the order of the real parts of $\lambda_n(\mathbf{k})$ changes, so this sorting method is not effective.

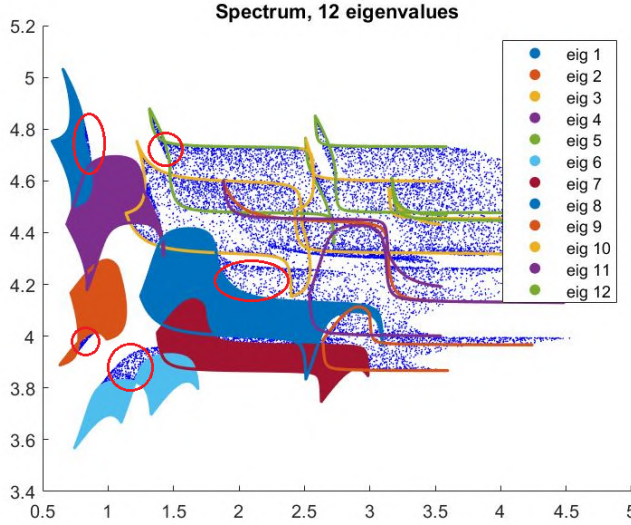


However, since \mathbf{k} varies continuously, the order of the vector obtained at the next value of \mathbf{k} can be reorganized to ensure that the values of $v_{\mathbf{k}}$ evolve continuously. Given v_{k_i} , I changed $v_{k_{i+1}}$ by the permutation of $v_{k_{i+1}}$ that minimize the norm of $v_{k_{i+1}} - v_{k_i}$. This requires `Neig!` calculations, which starts to take too much time when $\text{Neig} > 7$. In the previous picture, we have $\text{Neig} = 12$. I tried to first reorganize $v_{\mathbf{k}}(1 : 7)$ then $v_{\mathbf{k}}(6 : 12)$. It still works because if we look along a vertical line, we can see that no more than 7 eigenvalues are sharing the same real part. However, an error is made inside the red square, which prevents to fill up this mainly green loop.

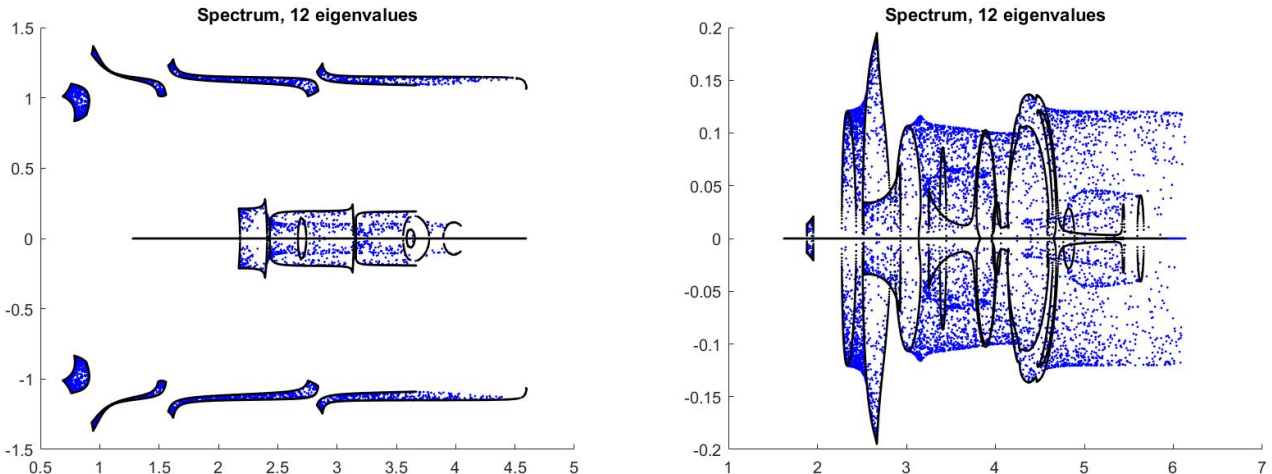


4 SOME IDEAS OF IMPROVEMENTS

A puzzling question now arises: Where do the points lying outside the filled areas come from?



If we draw $\lambda_n(\partial\mathcal{B}_{2D}^{\frac{1}{4}})$ for other potentials, it seems that it always gives us some of the boundaries of the spectrum.



$$V(x_1, x_2) = i \cos(x_1) \sqrt{x_2}$$

$$V(x_1, x_2) = \sqrt{x_1} + \frac{1}{2}i \cos(x_1) \sin(x_2)$$

We couldn't explain this phenomenon for all types of potential but we found an explanation when $V(x_1, x_2) = V_1(x_1) + V_2(x_2)$. In this case (see appendix C), the spectrum of H is the sum of two spectra of one-dimensional operators:

$$\sigma(H) = \sigma(H^{V_1}) + \sigma(H^{V_2})$$

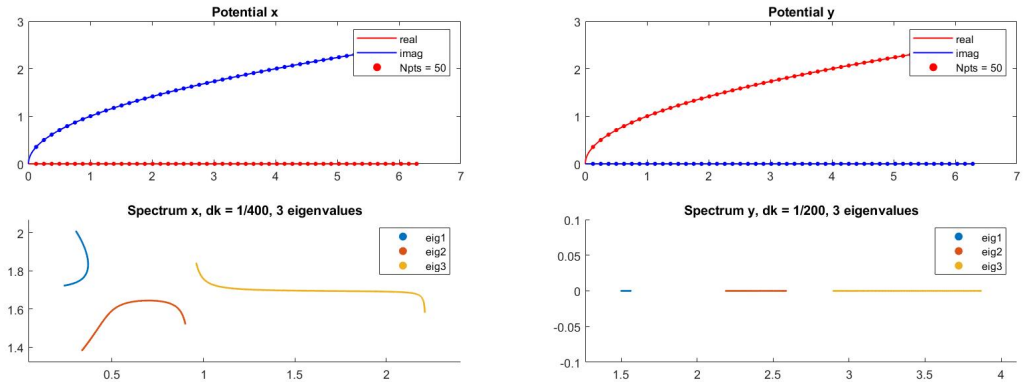
4 SOME IDEAS OF IMPROVEMENTS

If we note $\lambda_n^{V_1}(k_1)$ the eigenvalues of H^{V_1} and $\lambda_m^{V_2}(k_2)$ the eigenvalues of $\sigma(H^{V_2})$, we can index the eigenvalues of H by $\mathbb{N}^* \times \mathbb{N}^*$ and we have:

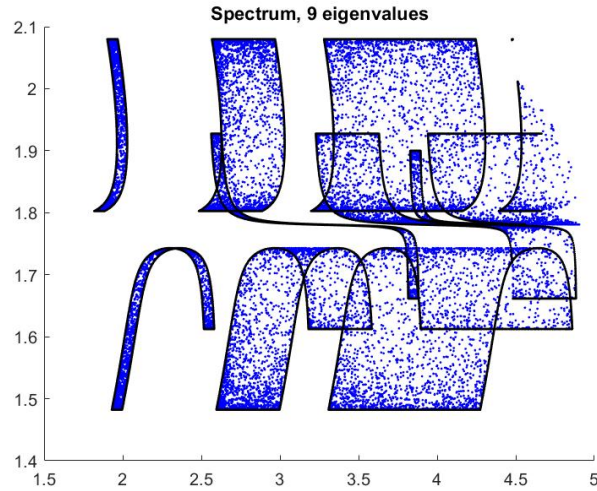
$$\lambda_{n,m}(k_1, k_2) = \lambda_n^{V_1}(k_1) + \lambda_m^{V_2}(k_2)$$

If we take V_2 real, each $\lambda_m^{V_2}(\mathcal{B}_{1D})$ will be a segment $[a_m, b_m]$ of the real axis.

The connected components $\lambda_{n,m}(\mathcal{B}_{2D})$ correspond to the area covered by $\lambda_n^{V_1}(\mathcal{B}_{1D})$ during a translation from a_m to b_m .



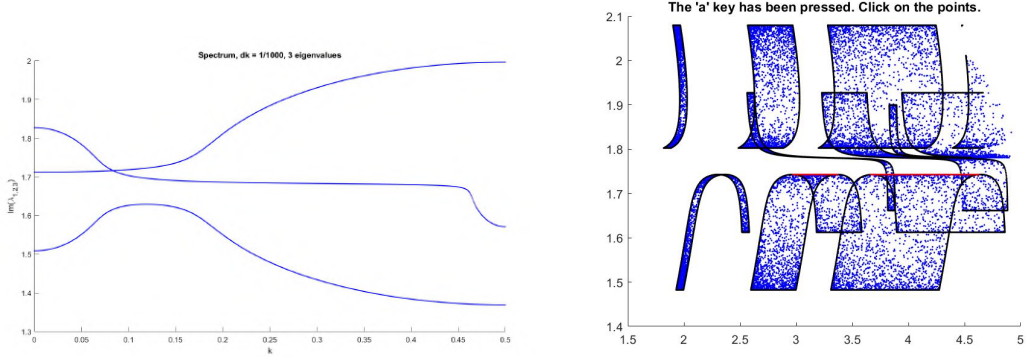
We can clearly identify the $\lambda_{n,m}(\mathcal{B}_{2D})$.



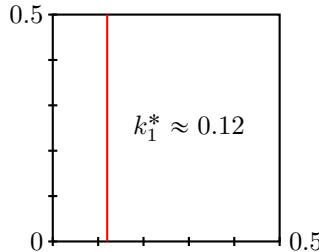
The black lines $\lambda_{1,m}(\partial\mathcal{B}_{2D}^{\frac{1}{4}})$ and $\lambda_{3,m}(\partial\mathcal{B}_{2D}^{\frac{1}{4}})$ give us all the boundaries of $\lambda_{1,m}(\mathcal{B}_{2D})$ and $\lambda_{3,m}(\mathcal{B}_{2D})$ because the imaginary parts of $\lambda_1^{V_1}(\cdot)$ and $\lambda_3^{V_1}(\cdot)$ are one-to-one.

4 SOME IDEAS OF IMPROVEMENTS

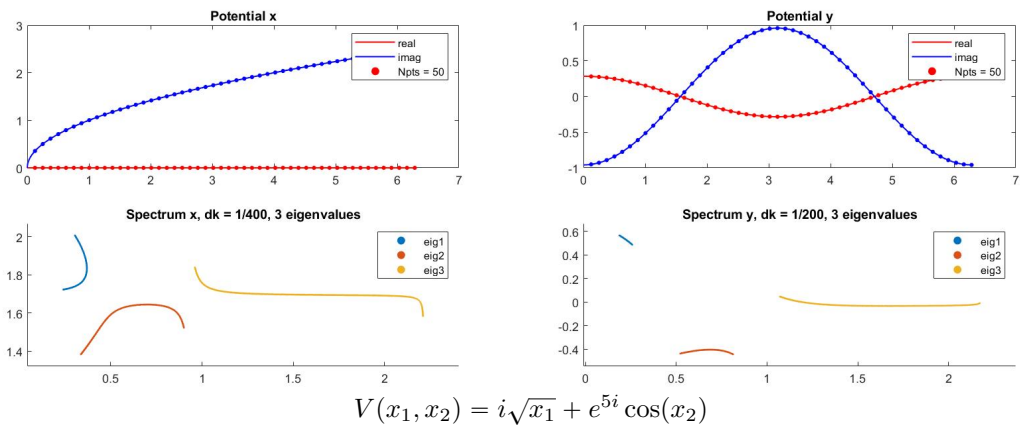
Let's find the value k_1^* for which the function $\Im(\lambda_2^{V_1}(\cdot))$ reaches its maximum.

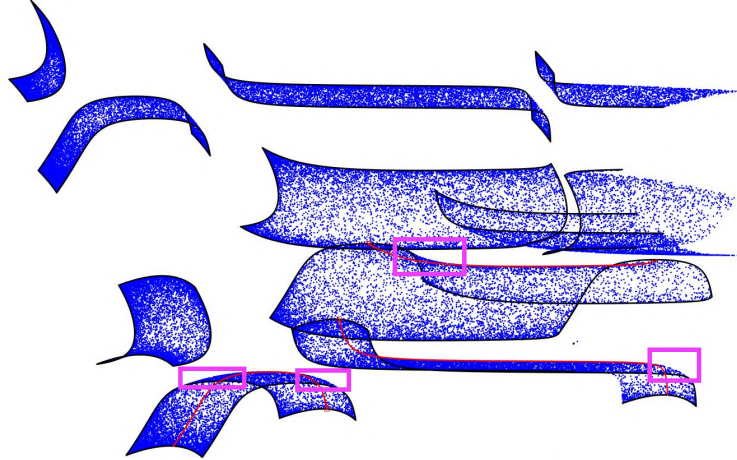


$k_1^* \approx 0.12$. If we plot $\lambda_{2,m}(k^*, \mathcal{B}_{1D})$, we get the missing boundaries at the top.
To get all the boundaries, we only used the following lines of the Brillouin zone:

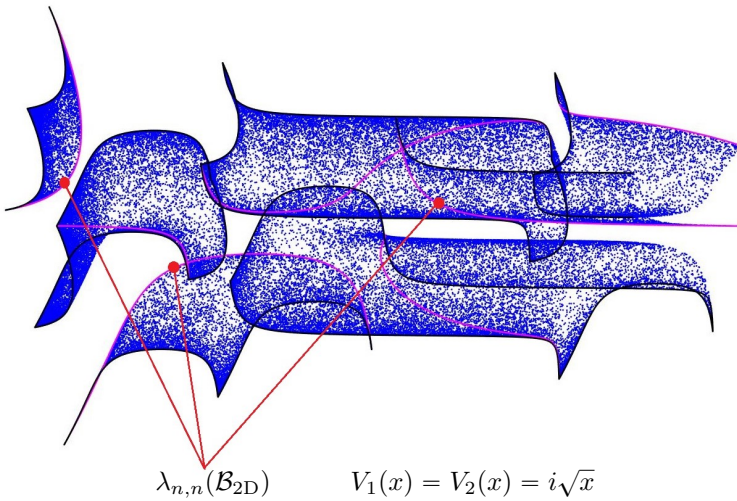


If we now take a complex potential V_2 , the shape of the $\lambda_{n,m}(\mathcal{B}_{2D})$ is much more complicated. In this case, we can't get the missing top boundaries by translating one point $\lambda_n^1(k_1^*)$ along $\lambda_m^2(\mathcal{B}_{1D})$ (which corresponds to the image of a vertical line under the $\lambda_{n,m}(\cdot, \cdot)$ function) or by translating one point $\lambda_m^2(k_1^*)$ along $\lambda_n^1(\mathcal{B}_{1D})$ (which corresponds to the image of a horizontal line under the $\lambda_{n,m}(\cdot, \cdot)$ function).



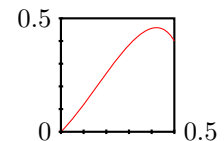


In red are plotted the lines that should be used to get the missing boundaries by the previous method. It matches with the boundaries only on a certain length. Inside the pink rectangles, some points are still outside the red boundaries.



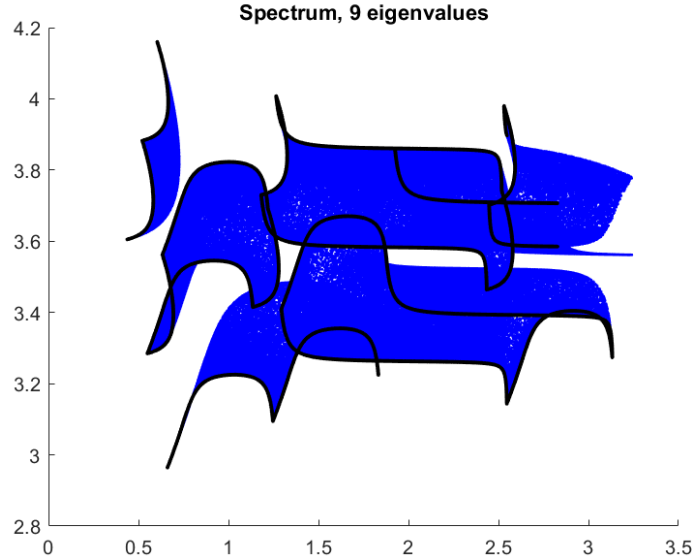
If we take $V_1 = V_2$, we notice that one of the boundaries of the $\lambda_{n,n}(B_{2D})$ blocks is always given by the image of the diagonal (plotted in magenta).

The diagonal is not a horizontal or vertical line but a straight one. It might be possible that in the case V_1 and V_2 complex, finding the boundaries of the $\lambda_{n,n}(B_{2D})$ blocks requires to cut the reduced Brillouin zone $B_{2D}^{\frac{1}{4}}$ with curved lines such as:



4 SOME IDEAS OF IMPROVEMENTS

I didn't have time to investigate that further, but knowing that the spectrum is the result of the sum of two one-dimensional spectra already enables us to identify the connected components and assume that a boundary drawn by random points is reliable.



By adjusting the thickness of the points and the scale, a continuous rendering can be achieved in less than 15 minutes of computation. The black lines allow us to guess the underlying curve translations, ensuring that the two holes in the center are real and not artifacts of the random selection of \mathbf{k} values.

We didn't speak about the case of a real V in 2D because according to the Bethe-Sommerfeld conjecture (1934, proved by Parnovski in 2007), the spectrum contains a finite number of gaps.

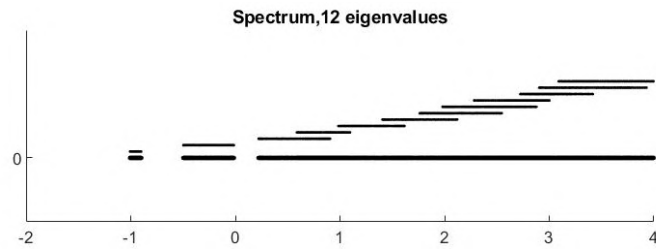


Illustration of the Bethe-Sommerfeld conjecture with $V(x_1, x_2) = \cos(x_1)\sqrt{x_2}$

By displaying each band $\lambda_n(\mathcal{B}_{2D})$ one above the other, we can see that they start to overlap from $n = 3$, unlike in dimension 1, where they are either disjoint or only touch at the endpoints.

4 SOME IDEAS OF IMPROVEMENTS

The generalization of the Bethe-Sommerfeld conjecture for a complex V could be a finite number of holes in its inside...

A Floquet theory

In the 1-dimensional case, our operator is:

$$H = -\frac{d}{dx^2} + V(x)$$

where $V : \mathbb{R} \rightarrow \mathbb{C}$ is a -periodic and bounded.

For each $\lambda \in \mathbb{C}$, the second-order differential equation:

$$-\frac{d}{dx^2}u + (V(x) - \lambda)u = 0 \quad (E_\lambda)$$

always have a solution space of dimension 2.

What is the relation between the behavior of the solutions of (E_λ) and the belonging or not of λ to the spectrum?

The domain of our operator is $H^2(\mathbb{R})$. In the selfadjoint case (V real), the spectrum is purely essential. As there is no eigenvector of H , there is no solution to the differential equation that lies in $H^2(\mathbb{R})$.

However, in the selfadjoint case, if one solution of (E_λ) is bounded in $\pm\infty$, we have $\lambda \in \sigma_{\text{ess}}(H)$. Indeed, if u is bounded in $\pm\infty$, it is possible to construct a Weyl sequence by using:

$$u_n(x) = \frac{1}{\sqrt{n}}\phi\left(\frac{x}{n}\right)u(x)$$

with $\phi \in \mathcal{D}(\mathbb{R})$ such that $\|\phi\|_{L^2(\mathbb{R})}$. (see (5))

For the non-selfadjoint case (V complex), it is much more complicated to give a definition of $\sigma_{\text{ess}}(H)$. But we will assume that we also have the property:

$$\lambda \in \sigma(H) \iff \text{One solution of } (E_\lambda) \text{ is bounded in } \pm\infty$$

The Floquet theory gives us that we can replace bounded by a certain form of periodicity, which is surprisingly more restrictive!

$$\begin{aligned} \lambda \in \sigma(H) &\iff \text{One non-zero solution of } (E_\lambda) \text{ satisfies } \psi(x+a) = \rho\psi(x) \quad \rho \in \mathbb{U} \\ &\iff \text{One non-zero solution of } (E_\lambda) \text{ satisfies } \psi(x+a) = e^{ika}\psi(x) \quad k \in [-\frac{\pi}{a}, \frac{\pi}{a}] \end{aligned}$$

This implies the useful spectral decomposition :

$$\sigma(H) = \bigcup_{k \in [-\frac{\pi}{a}, \frac{\pi}{a}]} \sigma(H_k)$$

However, this decomposition is not optimal. To reduce it to $k \in [0, \frac{\pi}{a}]$ we need to introduce the Hill discriminant. (see appendix B)

B HILL DISCRIMINANT

B Hill discriminant

For each $\lambda \in \mathbb{C}$, the second-order differential equation:

$$-\frac{d}{dx^2}u + (V(x) - \lambda)u = 0 \quad (E_\lambda)$$

always have a solution space of dimension 2. so we can find two functions that form a basis of the solution space.

Let's call them ψ_1^λ and ψ_2^λ and set their initial conditions: $\begin{cases} \psi_1^\lambda(0) = 0 \\ \psi_1'^\lambda(0) = 1 \end{cases} \quad \begin{cases} \psi_2^\lambda(0) = 1 \\ \psi_2'^\lambda(0) = 0 \end{cases}$

The Hill discriminant of H is a function of λ defined by:

$$\Delta(\lambda) = \psi_1^\lambda(a) + \psi_2'^\lambda(a)$$

We have seen in appendix A that:

$\lambda \in \sigma(H) \iff$ One non-zero solution of (E_λ) satisfies $\psi(x+a) = \rho \psi(x) \quad \rho \in \mathbb{U}$

Let's search for a solution of (E_λ) of the form $\psi(x+a) = \rho \psi(x)$ with ρ in \mathbb{C} . We decompose

$$\psi(x) = c_1 \psi_1(x) + c_2 \psi_2(x)$$

The equation (E_λ) is invariant by translation of a due to the a -periodicity of V . So $\psi_1(x+a)$ and $\psi_2(x+a)$ are also solutions:

$$\begin{cases} \psi_1(x+a) = A_{11}\psi_1(x) + A_{12}\psi_2(x) \\ \psi_2(x+a) = A_{21}\psi_1(x) + A_{22}\psi_2(x) \end{cases}$$

If we want $\psi(x+a)$ to be equal to $\rho\psi(x)$, we need to satisfy:

$$\begin{cases} \rho A_{11}c_1 + A_{21}c_2 = \rho c_1 \\ \rho A_{12}c_1 + A_{22}c_2 = \rho c_2 \end{cases} \iff \begin{cases} \rho(A_{11} - \rho)c_1 + A_{21}c_2 = 0 \\ \rho A_{12}c_1 + (A_{22} - \rho)c_2 = 0 \end{cases}$$

This equality holds for some non-zero c_1 and c_2 if and only if:

$$\det \begin{pmatrix} A_{11} - \rho & A_{21} \\ A_{12} & A_{22} - \rho \end{pmatrix} \neq 0$$

i.e. $\rho^2 - (A_{11} + A_{22})\rho + \det(A) = 0$ with $A = \begin{pmatrix} A_{11} & A_{21} \\ A_{12} & A_{22} \end{pmatrix}$

Due to the initial conditions of ψ_1^λ and ψ_2^λ , we get:
 $A_{11} = \psi_1^\lambda(a), A_{12} = \psi_1'^\lambda(a), A_{21} = \psi_2^\lambda(a), A_{22} = \psi_2'^\lambda(a)$.

B HILL DISCRIMINANT

So $\det(A)$ is then equal to the Wronskian of ψ_1^λ and ψ_2^λ in a . We use Liouville's formula of the Wronskian:

$$W(a) = W(0) \exp \left(\int_0^a \text{Tr}(C_\lambda(\tau)) d\tau \right),$$

$C_\lambda(x)$ is the matrix used to transform (E_λ) into a first-order differential equation.

Setting $U = \begin{pmatrix} u \\ u' \end{pmatrix}$, we have

$$U' = C_\lambda(x) \quad \text{with} \quad C_\lambda(x) = \begin{pmatrix} 0 & 1 \\ V(x) - \lambda & 0 \end{pmatrix}$$

Thus $\text{Tr}(C_\lambda(\tau)) = 0 \quad \forall \tau$ and $W(a) = W(0) = 1$.

Finally, we know that ρ satisfies: $\rho^2 - \Delta(\lambda)\rho + 1 = 0$

This equation has 2 solutions ρ_1 and ρ_2 in \mathbb{C} .

- If $|\Delta(\lambda)| > 2$ then

$$\begin{cases} \rho_1, \rho_2 \in \mathbb{R} \\ \rho_1 \neq \rho_2 \\ \rho_1 \rho_2 = 1 \end{cases} \implies \lambda \notin \sigma(H)$$

- If $|\Delta(\lambda)| \leq 2$ then

$$\begin{cases} \rho_1, \rho_2 \in \mathbb{C} \\ \rho_1 = \rho_2^* \\ \rho_1 \rho_2 = 1 \end{cases} \implies \rho_1, \rho_2 \in \mathbb{U} \implies \lambda \in \sigma(H)$$

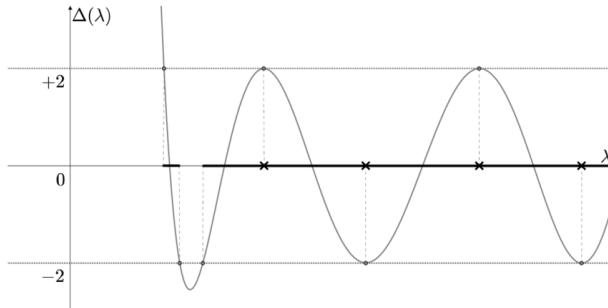
For $|\Delta(\lambda)| \leq 2$, if we wrote $\rho_1 = e^{ika}$ and $\rho_2 = e^{-ika}$, we get:

$$e^{ika} + e^{-ika} = \Delta(\lambda) \iff 2 \cos(ka) = \Delta(\lambda)$$

The Hill discriminant has the following properties:

- (i) $|\Delta(\lambda)| \leq 2 \iff \lambda \in \sigma(H)$
- (ii) $|\Delta(\lambda)| - 2 \cos(ka) = 0 \iff \lambda \in \sigma(H_k)$

(ii) allows us to optimize the spectral decomposition explained in appendix A.



C Special Case in 2D: $V(x_1, x_2) = V_1(x_1) + V_2(x_2)$

Our Hill operator of domain $H^2(\mathbb{R}^2)$ is :

$$H = -\Delta + V_1(x_1) + V_2(x_2) = -\frac{d}{dx_1^2} - \frac{d}{dx_2^2} + V_1(x_1) + V_2(x_2)$$

where $\begin{cases} V_1 \text{ is } a\text{-periodic and bounded} \\ V_2 \text{ is } b\text{-periodic and bounded} \end{cases}$

We are going to prove $\sigma(H) = \sigma(H^{V_1}) + \sigma(H^{V_2})$ with H^{V_i} of domain $H^2(\mathbb{R})$.

$$H^{V_i} = -\frac{d}{dx_i^2} + V_i(x_i)$$

The Floquet-Bloch transform gives us:

$$\sigma(H) = \bigcup_{(k_1, k_2) \in [0, \frac{2\pi}{a}] \times [0, \frac{2\pi}{b}]} \sigma(H_{k_1, k_2})$$

Because of the optimization of this transform proved in 1D in appendix B and the spectral decomposition of H in two 1D-problems, we get:

$$\sigma(H) = \bigcup_{(k_1, k_2) \in [0, \frac{\pi}{a}] \times [0, \frac{\pi}{b}]} \sigma(H_{k_1, k_2})$$

Only a quarter of the Brillouin zone is needed!

Proof. • Let's start with the inclusion: $\sigma(H^{V_1}) + \sigma(H^{V_2}) \subset \sigma(H)$

Given $\lambda \in \sigma(H^{V_1})$ and $\mu \in \sigma(H^{V_2})$, there exists k_λ and k_μ such that: $\begin{cases} \lambda \in \sigma(H_{k_\lambda}^{V_1}) \\ \mu \in \sigma(H_{k_\mu}^{V_2}) \end{cases}$

Let's take u_1 an eigenvector in $H^2([0, a])$ of $H_{k_\lambda}^{V_1}$ associated with the eigenvalue λ and u_2 an eigenvector in $H^2([0, b])$ of $H_{k_\mu}^{V_2}$ associated with the eigenvalue μ .

$$\begin{cases} -\frac{d}{dx^2} u_1 + V_1(x) u_1 = \lambda u_1 \\ u_1(a) = e^{ika} u_1(0) \\ u'_1(a) = e^{ika} u'_1(0) \end{cases} \quad \begin{cases} -\frac{d}{dx^2} u_2 + V_2(x) u_2 = \mu u_2 \\ u_2(b) = e^{ikb} u_2(0) \\ u'_2(b) = e^{ikb} u'_2(0) \end{cases}$$

If we set $u(x_1, x_2) = u_1(x_1)u_2(x_2)$, we have $u \in H^2([0, a] \times [0, b])$ and:

$$\begin{cases} -\frac{d}{dx_1^2} u - \frac{d}{dx_2^2} u + V_1(x_1)u + V_2(x_2)u = (\lambda + \mu)u \\ u(a, \cdot) = e^{ika} u(0, \cdot) \\ u(\cdot, b) = e^{ikb} u(\cdot, 0) \\ u'(a, \cdot) = e^{ika} u'(0, \cdot) \\ u'(\cdot, b) = e^{ikb} u'(\cdot, 0) \end{cases}$$

So $(\lambda + \mu) \in \sigma(H_{k_\lambda, k_\mu}) \subset \sigma(H)$.

C SPECIAL CASE IN 2D: $V(x_1, x_2) = V_1(x_1) + V_2(x_2)$

- Now we have to prove the reciprocal inclusion: $\sigma(H) \subset \sigma(H^{V_1}) + \sigma(H^{V_2})$

Suppose that $Hu = -\Delta u + (V_1(x_1) + V_2(x_2))u$ and that we seek a solution of the equation $Hu - \lambda u = 0$, of the form

$$u(x, y) = \sum_{n,m=1}^{\infty} c_{nm} X_n(x_1) Y_m(x_2),$$

in which $\{X_n \mid n \in \mathbb{N}\}$ and $\{Y_m \mid m \in \mathbb{N}\}$ are linearly independent functions that vanish only at discrete points. Provided the differentiated series converges locally uniformly, we have by direct formal calculation

$$(H - \lambda)u = \sum_{n,m=1}^{\infty} X_n(x_1) Y_m(x_2) \left[\frac{-X_n''(x_1) + V_1(x_1)X_n(x_1)}{X_n(x_1)} + \frac{-Y_m''(x_2) - \lambda V_2(x_2)Y_m(x_2)}{Y_m(x_2)} \right].$$

We deduce that the equation $(H - \lambda)u = 0$ can hold only if

$$\frac{-X_n''(x_1) + V_1(x_1)X_n(x_1)}{X_n(x_1)} + \frac{-Y_m''(x_2) - \lambda V_2(x_2)Y_m(x_2)}{Y_m(x_2)} = 0, \quad n, m \in \mathbb{N},$$

which in particular means that for some constant c independent of n and m we have

$$\frac{-X_n''(x_1) + V_1(x_1)X_n(x_1)}{X_n(x_1)} = c, \quad \frac{-Y_m''(x_2) - \lambda V_2(x_2)Y_m(x_2)}{Y_m(x_2)} = -c.$$

In order for X_n to be nontrivial it is necessary that $c =: \lambda_{n_1}^{V_1}$ be an eigenvalue of $-\frac{d^2}{dx_1^2} + V_1(x_1)$ (with appropriate boundary conditions). In order for Y_m to be nontrivial it is necessary that $\lambda - c =: \lambda_{n_2}^{V_2}$ be an eigenvalue of $-\frac{d^2}{dx_2^2} + V_2(x_2)$ (with appropriate boundary conditions). For the product $X_n Y_m$ to be nontrivial, both of these equations must hold. Adding the two equations we find that $\lambda = \lambda_{n_1}^{V_1} + \lambda_{n_2}^{V_2}$. □

Many thanks to M. Marletta for the writing of this page.

D Kronecker product

If \mathbf{A} is an $m \times n$ matrix and \mathbf{B} is a $p \times v$ matrix, then the Kronecker product $\mathbf{A} \otimes \mathbf{B}$ is the $pm \times vn$ block matrix:

$$\mathbf{A} \otimes \mathbf{B} = \begin{pmatrix} A_{11} \cdot \mathbf{B} & \dots & A_{1n} \cdot \mathbf{B} \\ \vdots & \ddots & \vdots \\ A_{m1} \cdot \mathbf{B} & \dots & A_{mn} \cdot \mathbf{B} \end{pmatrix}$$

Proof. We are going to prove $\frac{\partial}{\partial x_2} = \tilde{\mathbf{D}} \otimes \mathbf{I}$. (same proof for $\frac{\partial^2}{\partial x_2^2}$)

We chose to arrange the values $v_{i,j}$ in the vector v^\rightarrow but we could also have used:

$$v^\uparrow = \begin{pmatrix} w_1^\uparrow \\ w_2^\uparrow \\ \vdots \\ w_N^\uparrow \end{pmatrix} \quad \text{where} \quad w_i^\uparrow = \begin{pmatrix} v_{1i} \\ v_{2i} \\ \vdots \\ v_{Ni} \end{pmatrix}$$

It is immediately clear that $\frac{\partial}{\partial x_2} v^\uparrow = (\mathbf{I} \otimes \tilde{\mathbf{D}}) v^\uparrow$. Moreover $v^\uparrow = \mathbf{P} v^\rightarrow$ with:

$$\mathbf{P} = \begin{pmatrix} \mathbf{E}^{11} & \dots & \mathbf{E}^{N1} \\ \vdots & \ddots & \vdots \\ \mathbf{E}^{1N} & \dots & \mathbf{E}^{NN} \end{pmatrix} \quad \text{where } \mathbf{E}^{ij} \text{ is the } N \times N \text{ matrix with } \mathbf{E}^{ij}(k,l) = \delta_{ik}\delta_{jl}$$

We have then $\frac{\partial}{\partial x_2} \mathbf{P} v^\rightarrow = (\mathbf{I} \otimes \tilde{\mathbf{D}}) \mathbf{P} v^\rightarrow$ so $\frac{\partial}{\partial x_2} v^\rightarrow = \mathbf{P}^{-1} (\mathbf{I} \otimes \tilde{\mathbf{D}}) \mathbf{P} v^\rightarrow$.

As $\mathbf{P}^{-1} = \mathbf{P}$:

$$\begin{aligned} \mathbf{P}^{-1} (\mathbf{I} \otimes \tilde{\mathbf{D}}) \mathbf{P} &= \begin{pmatrix} \mathbf{E}^{11} & \dots & \mathbf{E}^{N1} \\ \vdots & \ddots & \vdots \\ \mathbf{E}^{1N} & \dots & \mathbf{E}^{NN} \end{pmatrix} \begin{pmatrix} \tilde{\mathbf{D}} & & \\ & \ddots & \\ & & \tilde{\mathbf{D}} \end{pmatrix} \begin{pmatrix} \mathbf{E}^{11} & \dots & \mathbf{E}^{N1} \\ \vdots & \ddots & \vdots \\ \mathbf{E}^{1N} & \dots & \mathbf{E}^{NN} \end{pmatrix} \\ &= \begin{pmatrix} \mathbf{E}^{11} & \dots & \mathbf{E}^{N1} \\ \vdots & \ddots & \vdots \\ \mathbf{E}^{1N} & \dots & \mathbf{E}^{NN} \end{pmatrix} \begin{pmatrix} \tilde{\mathbf{D}}\mathbf{E}^{11} & \dots & \tilde{\mathbf{D}}\mathbf{E}^{N1} \\ \vdots & \ddots & \vdots \\ \tilde{\mathbf{D}}\mathbf{E}^{1N} & \dots & \tilde{\mathbf{D}}\mathbf{E}^{NN} \end{pmatrix} \\ &= \left(\sum_{k=1}^{k=N} \mathbf{E}^{ki} \tilde{\mathbf{D}} \mathbf{E}^{jk} \right)_{(i,j)} = \left(\tilde{d}_{ij} \sum_{k=1}^{k=N} \mathbf{E}^{kk} \right)_{(i,j)} \quad \text{given that } \mathbf{E}^{ab} \mathbf{A} \mathbf{E}^{cd} = a_{bc} \mathbf{E}^{ad} \\ &= \begin{pmatrix} \tilde{d}_{11} \mathbf{I} & \dots & \tilde{d}_{1N} \mathbf{I} \\ \vdots & \ddots & \vdots \\ \tilde{d}_{N1} \mathbf{I} & \dots & \tilde{d}_{NN} \mathbf{I} \end{pmatrix} = \tilde{\mathbf{D}} \otimes \mathbf{I} \end{aligned}$$

□

Bibliography

- (1) M. S. P. Eastham, *The spectral theory of periodic differential equations*, Texts in Mathematics (Edinburgh), Scottish Academic Press, 1973
- (2) N. W. Ashcroft and N. D. Mermin, *Solid State Physics*, Saunders Collage Publishing, 1976
- (3) L. N. Trefethen, *Spectral Methods in Matlab*, SIAM, Philadelphia, 2000
- (4) P. Kuchment, *An Overview of Periodic Elliptic Operators*, Bulletin of the American Mathematical Society, Volume 53, Number 3, July 2016
- (5) Anne-Sophie Bonnet-Ben Dhia, Christophe Hazard et Jean-François Mercier
Théorie Spectrale des Opérateurs Auto-Adjoints et Applications, 2023